nature biomedical engineering

ARTICLES

DOI: 10.1038/s41551-017-0137-2

Nanoparticle delivery of Cas9 ribonucleoprotein and donor DNA in vivo induces homology-directed DNA repair

Kunwoo Lee[1], Michael Conboy[2], Hyo Min Park[1], Fuguo Jiang[3], Hyun Jin Kim[2,4,5], Mark A. Dewitt[3,6], Vanessa A. Mackley[1,2], Kevin Chang[3], Anirudh Rao[3], Colin Skinner[2], Tamanna Shobha[2], Melod Mehdipour[2], Hui Liu[1], Wen-chin Huang[2], Freeman Lan[2], Nicolas L. Bray[3,6], Song Li[2], Jacob E. Corn[3,6], Kazunori Kataoka[4,5,7], Jennifer A. Doudna[3,6,8,9,10], Irina Conboy[2]* and Niren Murthy[2]*

Clustered regularly interspaced short palindromic repeats (CRISPR)–CRISPR associated protein 9 (Cas9)-based therapeutics, especially those that can correct gene mutations via homology-directed repair, have the potential to revolutionize the treatment of genetic diseases. However, it is challenging to develop homology-directed repair-based therapeutics because they require the simultaneous in vivo delivery of Cas9 protein, guide RNA and donor DNA. Here, we demonstrate that a delivery vehicle composed of gold nanoparticles conjugated to DNA and complexed with cationic endosomal disruptive polymers can deliver Cas9 ribonucleoprotein and donor DNA into a wide variety of cell types and efficiently correct the DNA mutation that causes Duchenne muscular dystrophy in mice via local injection, with minimal off-target DNA damage.

Gene-editing therapeutics based on the clustered regularly interspaced short palindromic repeats (CRISPR)–CRISPR associated protein 9 (Cas9) system have tremendous potential for treating genetic diseases[1–4]. Primarily, two types of gene-editing therapies are being considered for the CRISPR–Cas9 system: therapies based on non-homologous end joining, which permanently silence disease-causing genes by inducing indel mutations, and therapies based on homology-directed repair (HDR), which correct disease-causing gene mutations to their wild-type sequence. HDR-based therapies have the potential to cure the vast majority of genetic diseases because of this mechanism of action. There is therefore great interest in developing HDR-based therapeutics. However, gene editing via HDR in vivo is challenging because HDR requires the delivery of Cas9, guide RNA (gRNA) and donor DNA.

Gene therapy with adeno-associated viruses (AAVs) is currently the most advanced methodology for delivering Cas9 in vivo[5,6]. However, developing Cas9 therapeutics based on AAV delivery is challenging because a large fraction of the human population has pre-existing immunity towards AAV, making them ineligible for AAV-based therapies. In addition, AAV-based Cas9 delivery has the potential to cause significant off-target genomic damage due to the sustained expression of Cas9 (refs [7,8]). AAV also has a small packing size and multiple viruses are needed to deliver Cas9 ribonucleoprotein (RNP) and donor DNA in vivo, which decreases the HDR efficiency of AAV-based Cas9-delivery methods. Finally, although AAV-based Cas9 delivery has generated several exciting pre-clinical demonstrations in vivo[9–11], the viral titers needed to generate therapeutic levels of editing have been orders of magnitude higher than the clinically accepted levels.

There is therefore great interest in developing non-viral Cas9-based therapeutics that can induce HDR[12]. However, developing delivery vehicles that can induce HDR in vivo has been challenging because of the multiple components involved. The only non-viral demonstration of HDR in vivo has been via the hydrodynamic delivery of plasmid DNA that expresses Cas9, gRNA and donor DNA[13]. The translational potential of hydrodynamic-based delivery of plasmids is unclear because of the dramatic changes in blood pressure that it causes.

Direct delivery of the Cas9 RNP is also being considered as a therapeutic strategy for generating HDR and has tremendous promise for clinical translation[14] because of the established protocols for producing proteins on a large scale and for clinical use, and because of the well-characterized clinical track record of protein therapeutics. Delivery strategies have been developed for delivering the Cas9 RNP in vitro and in vivo[15–18]. Lipofectamine and polyethylenimine have been the most successful Cas9 RNP delivery vehicles and have been able to deliver Cas9 RNP into the ear and in tumours to knock-out genes via non-homologous end joining. However, the application of lipid products or polyethylenimine to induce HDR in vivo has not been successfully demonstrated and will be potentially problematic due to the challenges associated with delivering multiple macromolecules in vivo. Therefore, the development of

[1]GenEdit, Berkeley, CA 94720-0001, USA. [2]Department of Bioengineering, University of California, Berkeley, Berkeley, CA 94720, USA. [3]Department of Molecular and Cell Biology, University of California, Berkeley, Berkeley, CA 94720, USA. [4]Center for Disease Biology and Integrative Medicine, Graduate School of Medicine, The University of Tokyo, Tokyo 113-0033, Japan. [5]Department of Materials Engineering, Graduate School of Engineering, The University of Tokyo, Tokyo 113-0033, Japan. [6]Innovative Genomics Initiative, University of California, Berkeley, Berkeley, CA 94720, USA. [7]Innovation Center of NanoMedicine, Institute of Industry Promotion-KAWASAKI, Kawasaki 210-0821, Japan. [8]Howard Hughes Medical Institute, University of California, Berkeley, Berkeley, CA 94720, USA. [9]Department of Chemistry, University of California, Berkeley, Berkeley, CA 97420-1460, USA. [10]Lawrence Berkeley National Laboratory, Berkeley, CA 94720, USA. Kunwoo Lee, Michael Conboy and Hyo Min Park contributed equally to this work. *e-mail: iconboy@berkeley.edu; nmurthy@berkeley.edu

vehicles that can simultaneously deliver Cas9 RNP and donor DNA and induce HDR in vivo remains a central problem in the field of therapeutic gene editing.

In this report, we present such a vehicle, which we name CRISPR–Gold. CRISPR–Gold can directly deliver Cas9 RNP and donor DNA in vivo via local administration and induce HDR. CRISPR–Gold is composed of gold nanoparticles (GNPs) conjugated with DNA, which are complexed with donor DNA, Cas9 RNP and the endosomal disruptive polymer poly(*N*-(*N*-(2-aminoethyl)-2-aminoethyl) aspartamide) (PAsp(DET)) (Fig. 1). CRISPR–Gold is designed to be internalized by cells via endocytosis due to the cationic PAsp(DET), which complexes the components of CRISPR–Gold[19,20]. After endocytosis, the PAsp(DET) polymer on CRISPR–Gold triggers endosomal disruption and causes the release of CRISPR–Gold into the cytoplasm (Fig. 1). Importantly, once in the cytoplasm, glutathione releases the DNA from the gold core of CRISPR–Gold, which causes the rapid release of Cas9 RNP and donor DNA[21].

Results and discussion

Design and synthesis of CRISPR–Gold. Non-viral gene editing via HDR requires the development of materials that can simultaneously deliver Cas9 RNP and donor DNA into cells. A key challenge in delivering both proteins and nucleic acids into cells is developing materials that can simultaneously complex both classes of macromolecules. CRISPR–Gold addresses this problem by taking advantage of the ability of Cas9 to bind gRNA and its affinity to the donor DNA coating the GNPs[22,23]. In addition, GNPs bind a large variety of proteins via non-specific electrostatic forces and could also have affinity for Cas9 RNP[24,25]. GNPs were selected as the core of CRISPR–Gold because they can be coated with a densely packed layer of DNA and because GNPs are taken up by a variety of different cell types[21,26–28]. The synthesis of CRISPR–Gold is shown in Fig. 2a and Supplementary Fig. 1. The first step in the synthesis was the facile reaction of thiol-terminated DNA with GNPs, followed by hybridization with the donor DNA. Cas9 RNP was then adsorbed onto the particles via the binding affinity of Cas9 RNP to the DNA loaded onto the GNPs and its potential non-specific affinity for GNPs. A layer of silica was then deposited onto the nanoparticles to increase the negative charge density and then finally complexed with the cationic endosomal disruptive polymer PAsp(DET)[29]. The synthesis of CRISPR–Gold was monitored using absorbance analysis, transmission electron microscopy (TEM) and dynamic light scattering (DLS) (Fig. 2b and Supplementary Figs. 2 and 3). The adsorption of the silica and the complexation of PAsp(DET) were monitored by zeta potential analysis. Large changes in the zeta potential of the CRISPR-Gold intermediates occurred after silica adsorption and PAsp(DET) complexation, demonstrating that they were bound to CRISPR–Gold (Fig. 2c). TEM analysis of CRISPR–Gold indicated that 5 min after formulation, it was composed of single GNPs. The structure of CRISPR–Gold was dynamic and aggregation was observed after 30 min, presumably due to interparticle electrostatic interactions.

Analysis of CRISPR–Gold complexes with Cas9 RNP. The ability of CRISPR–Gold to complex Cas9 RNP was investigated. CRISPR–Gold was synthesized following the procedures described above and the particles were purified via spin filtration through a 300 kDa molecular weight cut-off filter, washed and analysed via gel electrophoresis. The percentage of Cas9 RNP bound to the GNPs was determined by comparing the recovered Cas9 with the original amount of Cas9 mixed with the particles. Figure 2d demonstrates that CRISPR–Gold had a 61.5% encapsulation efficiency for complexing Cas9 RNP and thus has the complexation efficiency needed for developing Cas9 delivery vehicles. In addition, the activity of Cas9 RNP complexed to CRISPR–Gold was investigated. The enzymatic activity of Cas9 RNP released from CRISPR–Gold was examined by assaying its ability to cleave target DNA. Cas9-mediated DNA cleavage was analysed via gel electrophoresis[30]. Cas9 RNP released from CRISPR–Gold was still active and cleaved target template DNA (Supplementary Fig. 4). We also performed binding experiments with Cas9 RNP and unmodified GNPs and observed that Cas9 RNP bound unmodified GNPs, but the binding was unstable and did not survive multiple wash cycles (Supplementary Fig. 5).

Investigation of the ability of CRISPR–Gold to induce HDR in HEK cells. We performed HDR experiments on HEK293 (HEK, human embryonic kidney) cells expressing the blue fluorescent protein (BFP) to investigate the ability of CRISPR–Gold to induce HDR in cells[31]. CRISPR–Gold containing a single-stranded donor oligonucleotide to convert the BFP gene into a green fluorescent protein (GFP) gene and gRNA to cut the BFP gene were synthesized (as described in Supplementary Fig. 6). CRISPR–Gold was incubated with BFP-HEK cells (8 μg ml^{-1} Cas9 protein) and the level of HDR experienced by the BFP-HEK cells was determined by flow cytometry. Figure 3a shows that CRISPR–Gold induced 11.3% of the BFP-HEK cells to express GFP via HDR. This result was further confirmed by sequencing, which demonstrated that the GFP sequence in the edited cells exactly matched the donor DNA sequence (Supplementary Fig. 7). In addition, we performed experiments to determine the ratio of donor DNA to gRNA in CRISPR–Gold that generated the highest level of HDR in cells. CRISPR–Gold was made with various ratios of donor DNA to gRNA and was then incubated with BFP-HEK cells to measure the level of HDR induced. A 1:1 ratio of gRNA to donor DNA was determined to be optimal for inducing HDR (Supplementary Fig. 8; see Supplementary Fig. 9 for the fluorescent microscopy image).

In addition, we investigated the dose response of CRISPR–Gold, its cell culture toxicity and the mechanism by which CRISPR–Gold delivers Cas9 RNP and donor DNA. We observed that CRISPR–Gold had a maximum HDR efficiency at 8 μg ml^{-1} of Cas9, and that at doses above this level the HDR efficiency was lowered due to CRISPR–Gold-mediated cellular toxicity (see Supplementary Figs. 10 and 11). We also performed flow cytometry uptake experiments with fluorescence-labelled CRISPR–Gold (gRNA labelled)[32], in the presence of a panel of inhibitors to determine the mechanism by which cells internalize CRISPR–Gold. Figure 3b demonstrates that the caveolae/raft-dependent endocytosis inhibitors genistein and methyl-β-cyclodextrin dramatically reduced the cellular uptake of CRISPR–Gold, whereas the inhibitor of clathrin-mediated endocytosis, chlorpromazine, had no effect on uptake. Incubation of CRISPR–Gold with cells at 4 °C also inhibited uptake. Collectively, these experiments suggest that CRISPR–Gold is dependent on caveolae/raft-dependent endocytosis. Cellular uptake experiments with CRISPR–Gold were also performed with formulations that did not contain the polymer PAsp(DET). Figure 3b demonstrates that PAsp(DET) is essential for stimulating cellular uptake and suggests that it plays a key role in triggering endocytosis.

Finally, we performed HDR experiments with CRISPR–Gold, using the same panel of inhibitors described above, to investigate the relationship between cellular uptake and HDR efficiency. Figure 3c shows that genistein and methyl-β-cyclodextrin caused a significant reduction in HDR efficiency, whereas chlorpromazine had no effect on HDR efficiency, suggesting that CRISPR–Gold's ability to induce HDR in cells is largely dependent on caveolae/raft-dependent endocytosis.

HDR efficiency of CRISPR–Gold in primary cells and stem cells. The ability of CRISPR–Gold to induce HDR in a panel of therapeutically relevant cell types was tested to identify potential therapeutic applications of CRISPR–Gold. CRISPR–Gold's delivery efficiency was investigated in human embryonic stem cells, human induced

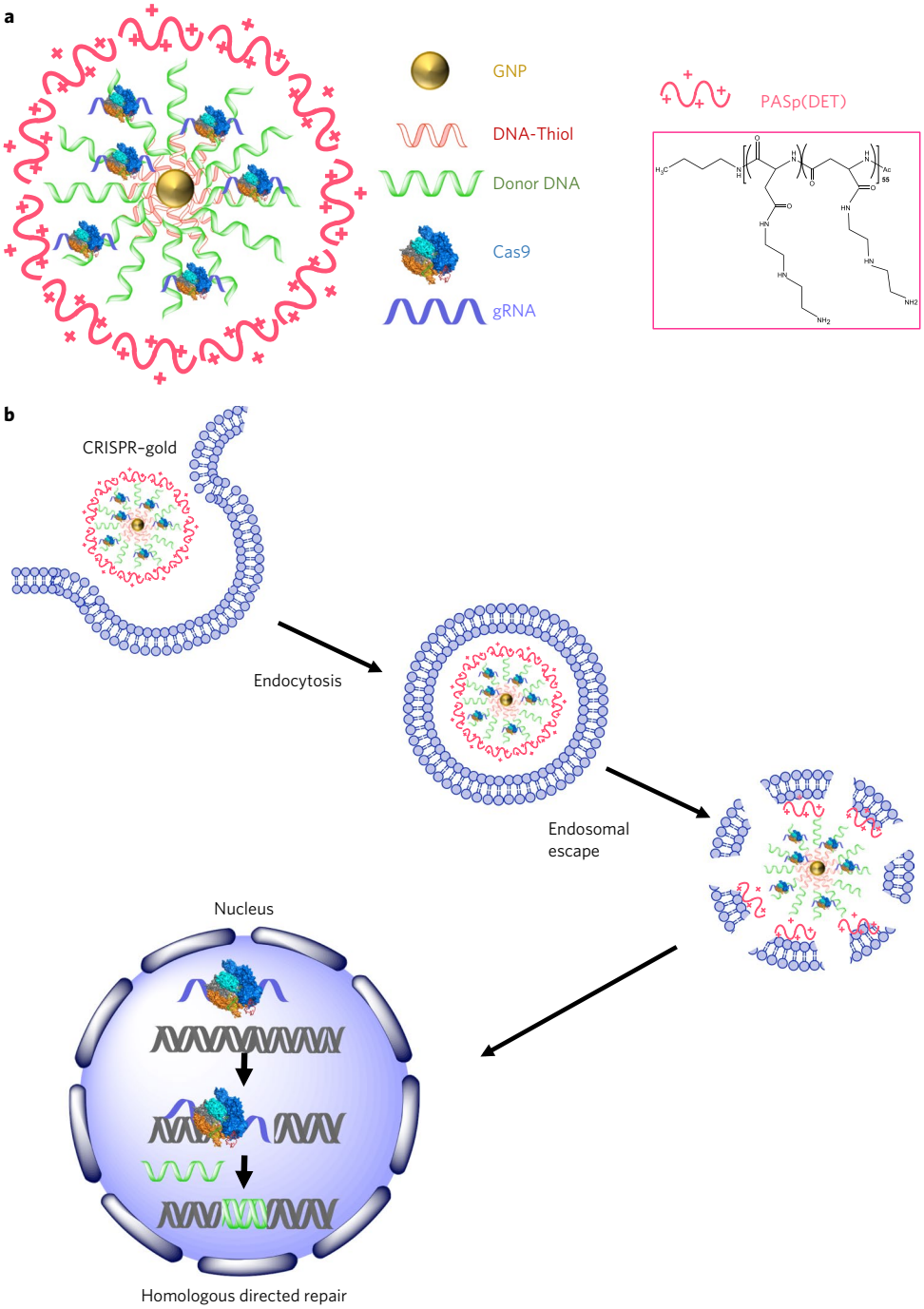

Fig. 1 | CRISPR–Gold can deliver Cas9 RNP and donor DNA in vivo and induce HDR. a, CRISPR–Gold is composed of 15 nm GNPs conjugated to thiol-modified oligonucleotides (DNA-Thiol), which are hybridized with single-stranded donor oligonucleotides and subsequently complexed with Cas9 RNP and the endosomal disruptive polymer PAsp(DET), where 'DET' is diethylenetriamine. **b**, CRISPR–Gold is internalized by cells in vitro and in vivo via endocytosis. This triggers endosomal disruption and releases Cas9 RNP and donor DNA into the cytoplasm. Nuclear delivery results in HDR.

pluripotent stem cells, primary bone-marrow-derived dendritic cells and primary myoblasts from *mdx* mice. CRISPR–Gold formulations were synthesized that were designed to edit the *CXCR4* gene or the dystrophin gene, and their ability to perform gene editing in cell culture was analysed. Figures 3d,e and 4 demonstrate that CRISPR–Gold was able to target CXCR4 in human embryonic stem cells, human induced pluripotent stem cells, bone-marrow-derived dendritic cells and the dystrophin gene in myoblasts with an HDR efficiency of between 3 and 4% (Supplementary Figs. 12–14)[8,30,33,34]. Importantly, CRISPR–Gold was significantly more effective at inducing HDR in these cell types and less toxic than either of the lipofectamine or nucleofection methods (Figs. 3 and 4)[35]. These results demonstrate that CRISPR–Gold can simultaneously deliver Cas9 protein, gRNA and donor DNA into a wide range of cells.

CRISPR–Gold-mediated gene editing in a reporter mouse model. We performed experiments on Ai9 mice to determine whether CRISPR–Gold could deliver the Cas9 RNP in vivo and generate double-stranded breaks. We used Ai9 mice for these experiments because gene deletions in the Ai9 DNA sequence result in the

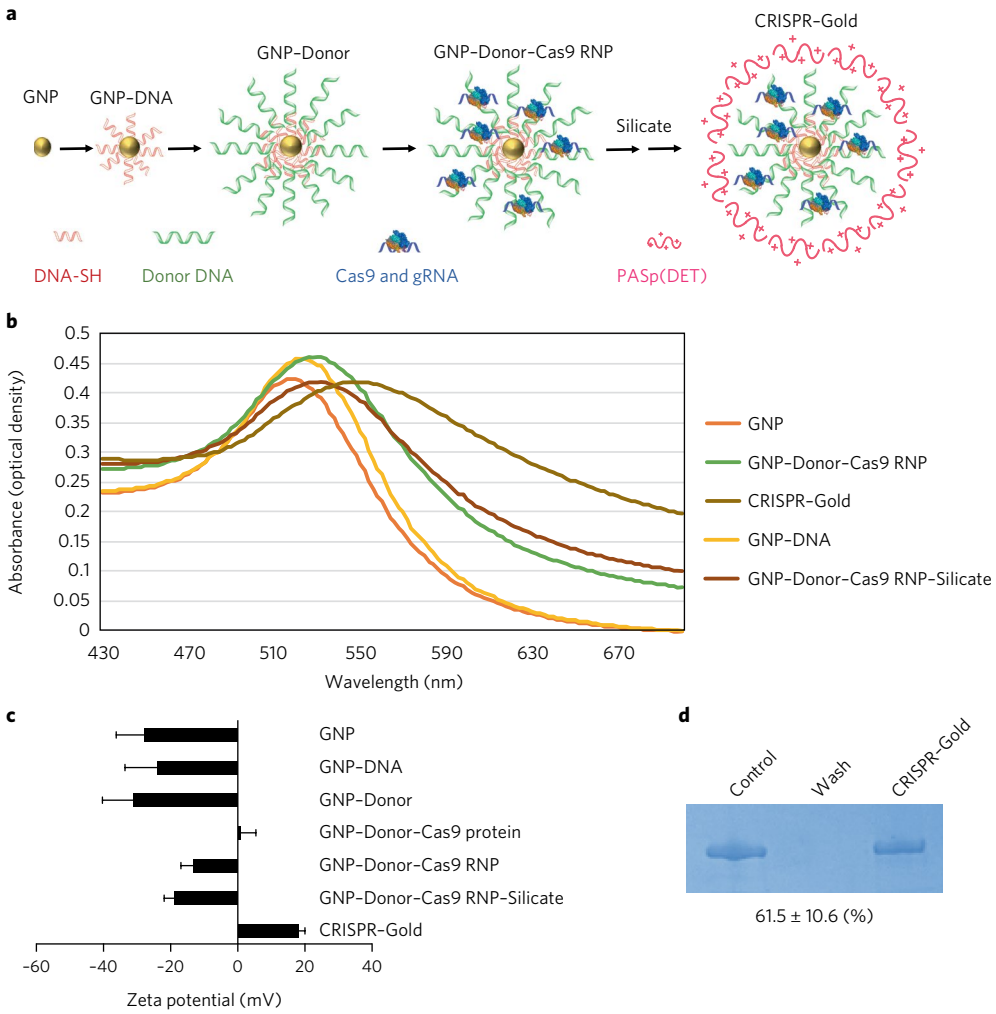

Fig. 2 | Synthesis and characterization of CRISPR–Gold. a, Synthesis of CRISPR–Gold. GNPs 15 nm in diameter were conjugated with a 5′ thiol modified single-stranded DNA (DNA-SH) and hybridized with single-stranded donor DNA. Cas9 and gRNA were loaded and then a silicate and PAsp(DET) polymer coating were added. **b**, Absorbance spectra analysis. The absorption maxima of CRISPR–Gold intermediates are red shifted as CRISPR–Gold is sequentially constructed. Unmodified GNPs had an absorbance peak at 518 nm. The peak shifted to 522 nm for GNP–DNA, 528 nm for GNP–DNA–Cas9 RNP and 546 nm for CRISPR–Gold. **c**, Zeta potential analysis. Zeta potential measurements were performed on CRISPR–Gold and all of the synthetic intermediates generated during the construction of CRISPR–Gold. Zeta potential changes demonstrated the sequential synthesis of CRISPR–Gold. Data are means ± s.e ($n = 3$). **d**, Cas9 loading analysis. CRISPR–Gold was formulated and the unbound Cas9 RNP was removed via spin filtration. Gel electrophoresis was performed on CRISPR–Gold and the sodium dodecyl sulfate gel was stained with Coomassie Brilliant Blue to quantify the amount of Cas9 RNP bound to CRISPR–Gold. The control represents the original amount of Cas9 RNP added to the CRISPR–Gold formulation. The wash represents the unbound Cas9 RNP removed by filtration.

expression of the fluorescent tdTomato protein, which can be monitored easily. Ai9 mice were given one intramuscular injection of CRISPR–Gold, designed to induce tdTomato fluorescence via gene deletion, and after two weeks, the expression of tdTomato was determined in 10 µm tibialis anterior muscle sections (see Supplementary Fig. 15 for more details). Figure 5 and Supplementary Fig. 16 demonstrate that CRISPR–Gold can deliver Cas9 RNP and generate gene deletions in Ai9 mice and that the gene-editing effect of CRISPR–Gold was observable millimetres away from the injection site. CRISPR–Gold can therefore efficiently deliver Cas9 RNP in vivo and edit genomic DNA.

Gene editing in mdx mice with CRISPR–Gold. CRISPR–Gold has numerous potential applications because of its ability to complex Cas9 RNP and donor DNA and deliver Cas9 RNP in vivo. We selected Duchenne muscular dystrophy (DMD) as an initial medical application for CRISPR–Gold. DMD is an early-onset lethal disease caused by mutations in the dystrophin gene. It is the most common congenital myopathy and approximately 30% of DMD patients have single base mutations or small deletions that could potentially be treated with HDR-based therapeutics[36]. Several therapeutic strategies have been developed to regenerate functional dystrophin in patients, ranging from exon skipping with antisense oligonucleotides to gene therapy with dystrophin minigenes[37–39]. However, despite significant efforts, the development of effective DMD therapies remains a major challenge. The disease is currently incurable and patients receive mostly palliative care, such as steroids, to diminish muscle inflammation. CRISPR–Cas9-based therapeutics have great potential for treating DMD because they can correct dystrophin gene mutations after a single injection and cure DMD. However, at present, the only gene-editing strategy available for treating DMD is based on non-homologous-end-joining-induced exon skipping, which generates a truncated form of dystrophin, with suboptimal functionality and used viral delivery of Cas9[9–11,40].

CRISPR–Gold was able to correct a point mutation in the dystrophin gene in primary myoblasts from the *mdx* mouse and induce the expression of dystrophin protein in myotubes that were differentiated from mdx myoblasts (Fig. 4a,b). Encouraged by these results, we investigated if CRISPR–Gold could correct the dystrophin mutation in *mdx* mice following an intramuscular injection

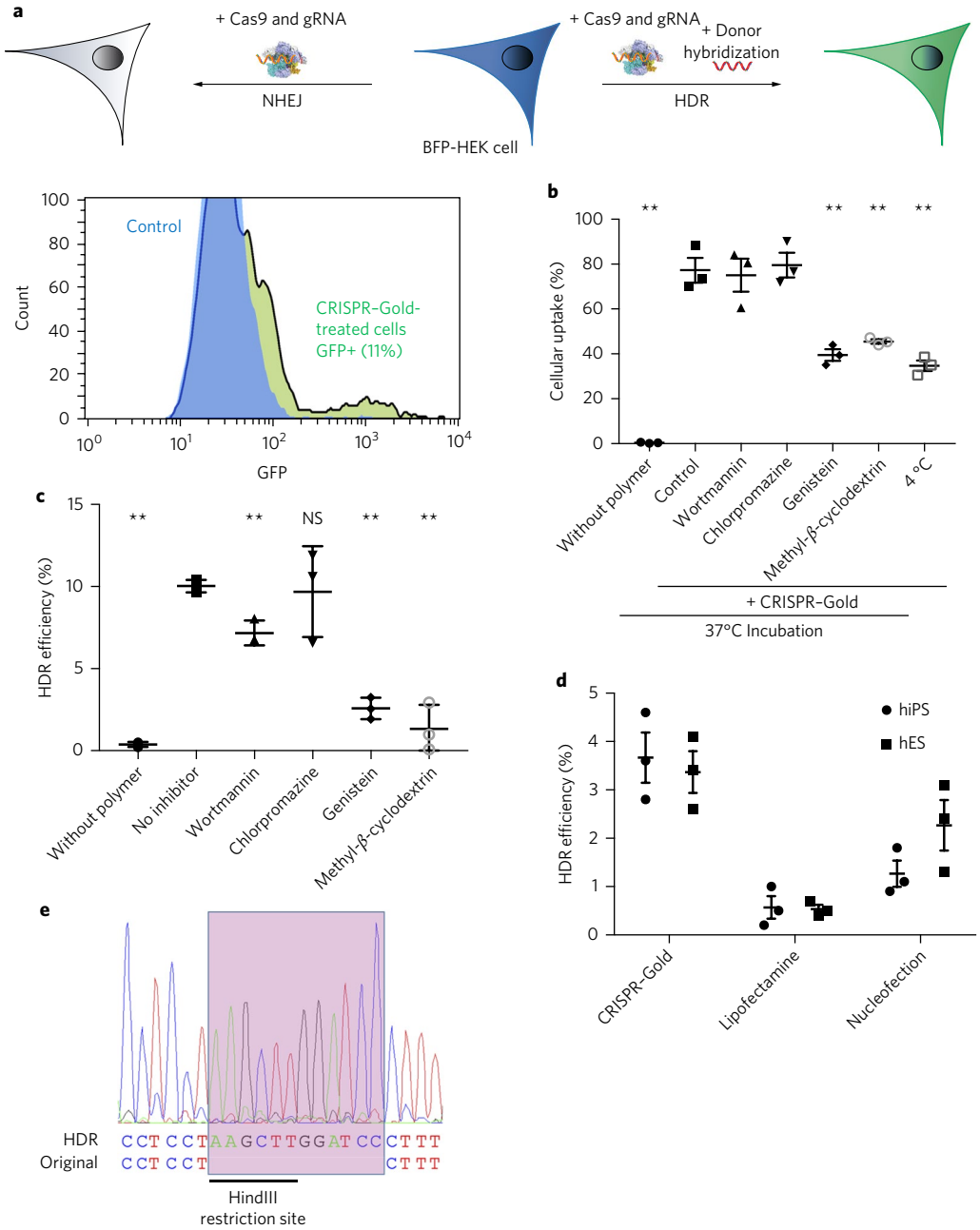

Fig. 3 | CRISPR–Gold induces HDR in vitro. a, CRISPR–Gold can induce HDR in BFP-HEK cells by delivering Cas9 RNP and donor DNA. In total, 11.3% of BFP-HEK cells were converted to GFP-expressing cells after treatment with CRISPR–Gold. GFP expression due to BFP sequence editing was determined by flow cytometry. **b**, The uptake of CRISPR–Gold in HEK293 cells is dependent on non-clathrin-mediated endocytosis. CRISPR–Gold containing Alexa647 labelled sgRNA was added to HEK293 cells and the uptake efficiency was measured using flow cytometry. Various inhibitors and low temperature were used to study the cellular uptake mechanism. The uptake of CRISPR–Gold without the PAsp(DET) polymer coating was also investigated. Genistein, methyl-β -cyclodextrin and 4 °C all significantly inhibited the uptake of CRISPR–Gold, whereas clathrin-based endocytosis inhibitors had no effect. Data are means ± s.e ($n = 3$). $^{**}P < 0.01$. **c**, Non-clathrin-mediated endocytosis plays a critical role in CRISPR–Gold-mediated HDR. The inhibitor of clathrin-mediated endocytosis, chlorpromazine, had minimal effects on CRISPR–Gold-mediated HDR, whereas the caveolae/raft-mediated endocytosis inhibitor methyl-β-cyclodextrin and genistein reduced CRISPR–Gold-mediated HDR by 80%. Data are means ± s.e ($n = 3$). $^{**}P < 0.01$; NS, not significant. **d**, CRISPR–Gold induces HDR in human embryonic stem cells (hES) and human induced pluripotent stem cells (hiPS) with higher efficiency than lipofectamine or nucleofection. Cells were treated with CRISPR–Gold containing a donor sequence with a HindIII cleavage site and a gRNA that targeted the *CXCR4* gene. The *CXCR4* gene was amplified by PCR and the HDR efficiency was determined by quantifying HindIII cleavage of the *CXCR4* PCR amplicon. Data are means ± s.e ($n = 3$). $P = 0.0066$ for hES samples and $P = 0.0023$ for hiPS samples (one-way analysis of variance). **e**, Sanger sequencing demonstrates that CRISPR–Gold induces HDR in hES. PCR of the *CXCR4* gene was performed on CRISPR–Gold-treated human embryonic stem cells and sequencing confirmed the presence of a 12-bp insertion (pink box).

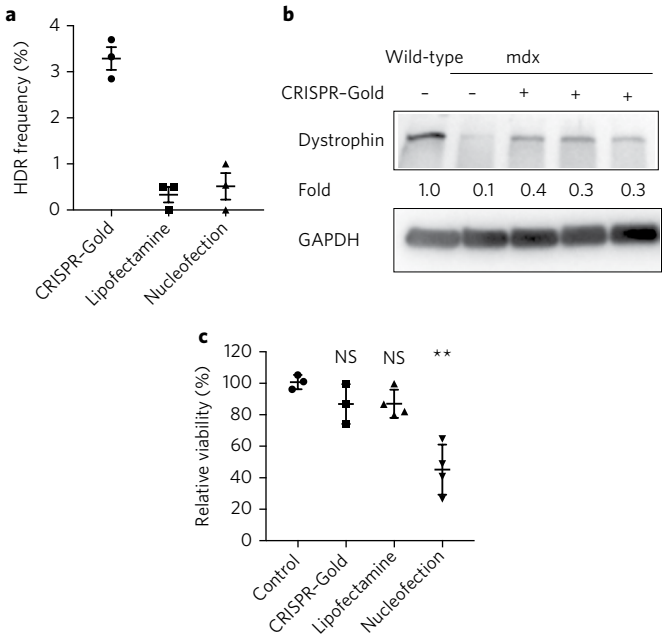

Fig. 4 | CRISPR-Gold induces HDR and promotes the expression of dystrophin protein in primary myoblasts. a, The dystrophin gene was edited with CRISPR-Gold in primary myoblasts from the *mdx* mouse. CRISPR-Gold corrected the nonsense mutation in the dystrophin gene of *mdx* myoblasts with an HDR efficiency of 3.3%, which is significantly higher than either nucleofection or lipofectamine. No correction was observed in the negative control, which was composed of CRISPR-Gold without gRNA (data not shown). Data are means ± s.e ($n=3$). $P=0.0002$ (one-way analysis of variance). **b**, Dystrophin protein was expressed in myotubes that were differentiated from CRISPR-Gold-edited primary *mdx* myoblasts. Western blot analysis was conducted to quantify the levels of dystrophin protein in muscle cells. The fold expression was determined by dividing the band pixel density of each group by the dystrophin band intensity from wild-type (C57.B6) myotubes ($n=1$). Glyceraldehyde 3-phosphate dehydrogenase (GAPDH) was used as a loading control. **c**, CRISPR-Gold caused minimal toxicity to primary myoblasts, whereas nucleofection caused significant toxicity. Primary *mdx* myoblasts were transfected and cell viability was measured two days after the transfections using the Cell Counting Kit-8. Data show the mean ± s.e viability relative to the control ($n=6$). *$P<0.05$; NS, not significant.

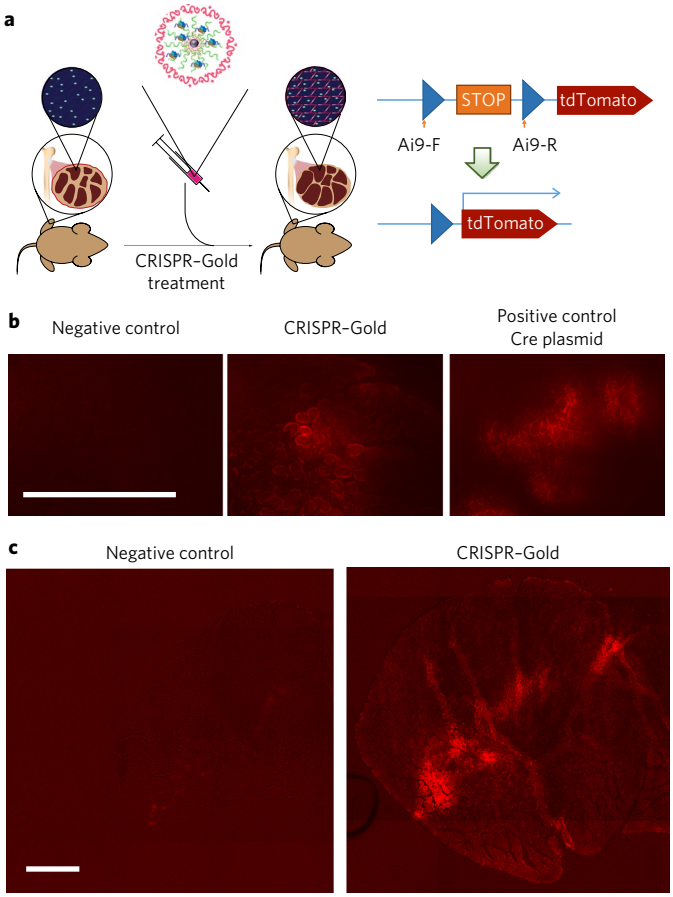

Fig. 5 | CRISPR-Gold induces gene editing in the muscle tissue of Ai9 mice **a**, CRISPR-Gold was injected into Ai9 mice and gene deletion of the stop sequence in the Ai9 gene was determined by tdTomato expression. **b**, Representative images of tdTomato fluorescence in the gastrocnemius muscle after a single CRISPR-Gold injection. A plasmid expressing Cre recombinase was injected with lipofectamine as a positive control. Scale bar: 500 μm. **c**, tdTomato expression was observed in a broad area of the muscle after injection with CRISPR-Gold. The entire tibialis anterior muscle cross-section image shows tdTomato expression after CRISPR-Gold injection. Scale bar: 500 μm.

(Fig. 6a). In the first studies, CRISPR–Gold (two different doses: 3 and 6 mg kg^{-1}) was injected into the gastrocnemius and tibialis anterior muscle of four-week-old *mdx* mice simultaneous with cardiotoxin (CTX), which activates the proliferation of muscle stem cells by muscle damage. After two weeks, the muscles were harvested and analysed for HDR in the dystrophin gene, the expression of dystrophin protein and muscle fibrosis. Remarkably, CRISPR–Gold was able to correct the mutated dystrophin gene in *mdx* mice to the wild-type sequence after a single injection and restore the expression of dystrophin protein in muscle tissue (Fig. 6b,c). Figure 6b demonstrates that CRISPR–Gold can induce HDR in the dystrophin gene. Specifically, 5.4% of the dystrophin gene in *mdx* mice was corrected back to the wild-type gene after CRISPR–Gold treatment, at 6 mg kg^{-1}, and this correction rate was approximately 18 times higher than treatment with Cas9 RNP and donor DNA by themselves, which had only a 0.3% correction rate (see Supplementary Fig. 17 for polymerase chain reaction (PCR) analysis). Robust dystrophin protein expression was also observed in 10 μm cryo-sections of the injected muscle tissue (Fig. 6c and Supplementary Figs. 18 and 19). In contrast, minimal levels of dystrophin expression were observed in the negative control, which was composed of Cas9 RNP and donor DNA injected without particles. In addition, Fig. 6d demonstrates that CRISPR–Gold-treated *mdx* mice had reduced levels of muscle fibrosis, which was indicative of better tissue health.

Muscle function in *mdx* mice treated with CRISPR–Gold. Encouraged by the above results, we performed additional experiments to determine the translational potential of CRISPR–Gold as a therapeutic approach for DMD under clinically relevant conditions (no CTX). *Mdx* mice were injected with CRISPR–Gold or the appropriate controls (without CTX) and a four-limb hanging test was performed on the mice to evaluate the therapeutic benefits of CRISPR–Gold. Promisingly, CRISPR–Gold was able to enhance animal strength and agility in *mdx* mice under these clinically relevant conditions. Specifically, CRISPR–Gold-treated *mdx* mice showed a two-fold increase in hanging time in the four-limb hanging test compared with *mdx* mice injected with scrambled CRISPR–Gold (Fig. 7a). CRISPR–Gold showed a 0.8% rate of HDR in the dystrophin gene without CTX (Supplementary Fig. 20). Additionally, deep sequencing analysis was performed to quantify the degree of off-target DNA damage CRISPR–Gold caused, which was found to be minimal and similar to the levels of sequencing error (0.005–0.2%; Fig. 7b). These

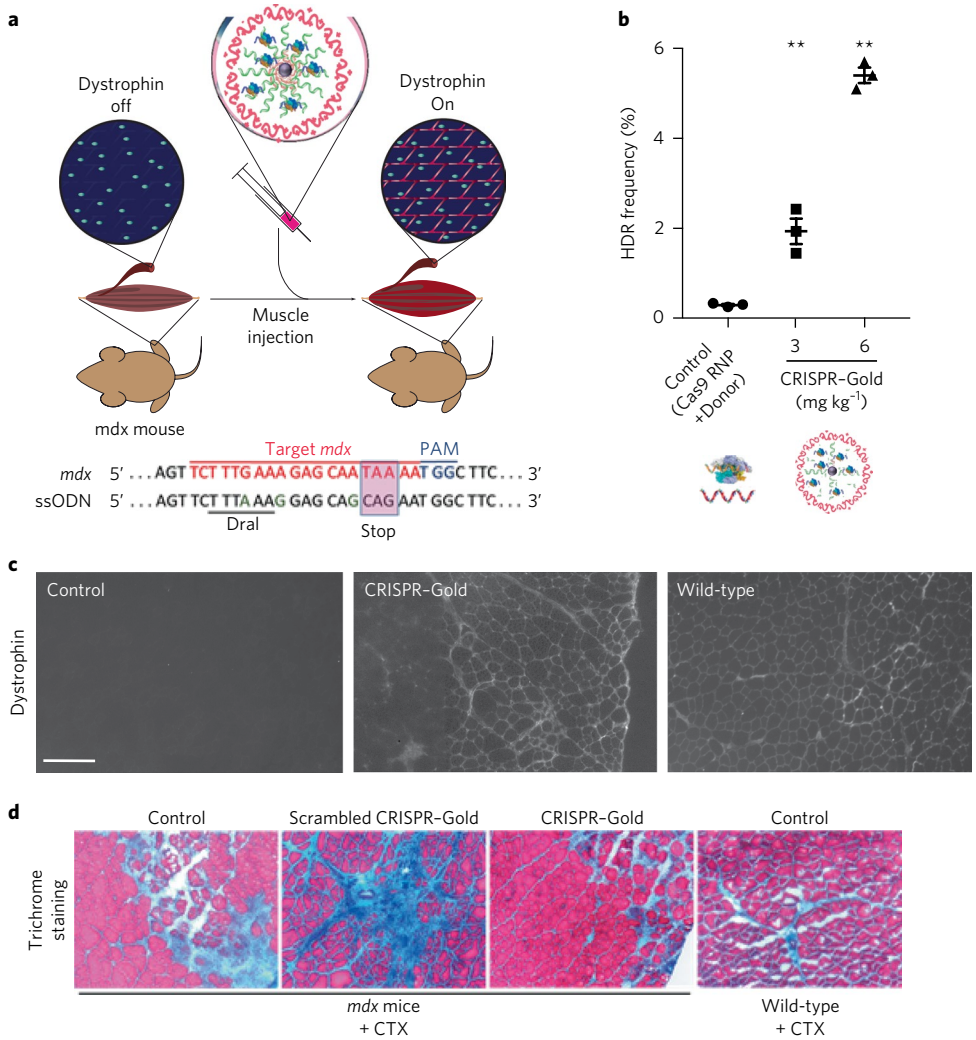

Fig. 6 | CRISPR-Gold promotes HDR in the dystrophin gene and dystrophin protein expression, and reduces muscle fibrosis in *mdx* mice, with CTX stimulation. a, CRISPR-Gold was injected into the hind leg muscle of eight-week-old *mdx* mice ($n = 3$) simultaneously with CTX. Two weeks later, the mice were sacrificed and analysed for dystrophin expression by immunofluorescence, for HDR by deep sequencing and for their degree of fibrosis. Bottom: dystrophin mutation sequence and donor DNA design. The donor DNA sequence designed to repair the nonsense mutation is marked in the pink box. The nucleotides marked in green (A, G and G) are silent mutations that prevent Cas9 activity on the edited sequence. ssODN, single stranded oligonucleotide. **b**, CRISPR-Gold-induced genome editing in the dystrophin gene was confirmed by deep sequencing. Deep sequencing of genomic DNA from muscle tissues injected with CRISPR-Gold revealed a 5.4% HDR efficiency. The negative control composed of Cas9 RNP and donor DNA had an HDR efficiency of only 0.3%. Data are means ± s.e ($n = 3$). $^{**}P < 0.01$. **c**, CRISPR-Gold-injected muscle of *mdx* mice showed dystrophin expression (immunofluorescence), whereas control *mdx* mice did not express dystrophin protein. Scale bar: 200 μm. **d**, CRISPR-Gold reduces muscle fibrosis in *mdx* mice. Trichrome staining was performed on the tibialis anterior muscle cryo-sectioned to 10 μm two weeks after an injection of CRISPR-Gold. CTX was co-injected in all three groups of *mdx* mice. Images were acquired at the areas of muscle injury and regeneration. Fibrotic tissue appears blue, while muscle fibres appear red. Wild-type mice treated with CTX were analysed five days after injection. The width of each image is 0.7 mm.

results demonstrate that CRISPR–Gold can induce HDR in muscle tissue with minimal off-target genomic damage, effectively edit the dystrophin mutation in *mdx* mice to the wild-type sequence and improve animal strength under clinically relevant conditions.

Analysis of CRISPR–Gold immunogenicity. Cas9 is a bacterial protein with potential immunogenicity. The immune response generated from CRISPR–Gold could therefore be problematic and limit its translational potential. To examine the possibility of an immune response to CRISPR–Gold, we injected CRISPR–Gold into the gastrocnemius muscle of *mdx* mice at 6 mg kg^{-1} of Cas9 protein. The systemic cytokine profile was analysed 24 h and two weeks after the CRISPR–Gold injection. Figure 7c,d shows that CRISPR–Gold did not cause an acute up-regulation of inflammatory cytokines in the plasma, thus suggesting the absence of a broad immune response towards CRISPR–Gold. In addition, plasma cytokine levels were stable two weeks after the injection (Supplementary Fig. 21). Furthermore, we stained the CRISPR–Gold-treated muscle tissue for CD45$^+$ and CD11b$^+$ cells, which are frequently found in muscle tissue undergoing inflammation and muscle regeneration[41]. We observed higher numbers of CD45$^+$ and CD11$^+$ leukocytes in tissues injected with CRISPR–Gold compared with controls (untreated mdx and wild-type muscles) (Supplementary Figs. 22–24). Macrophage-promoted clearance of nanoparticles and microparticles from muscle is expected, and intramuscular leukocytes are frequently found in the vicinity of Food and Drug Administration-approved biomaterials, such as poly(lactic-co-glycolic acid) microparticles[42].

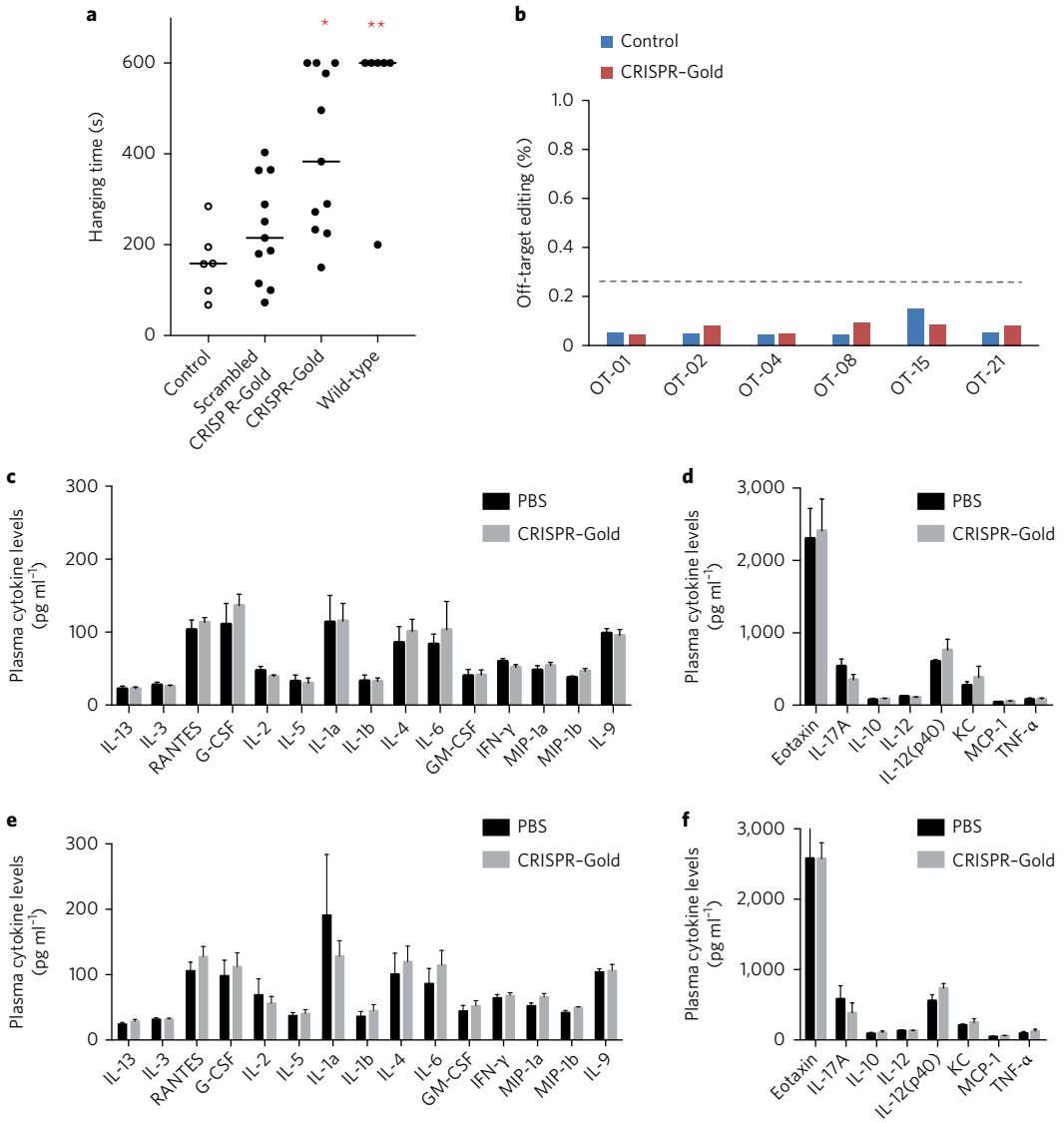

Fig. 7 | CRISPR–Gold-induced dystrophin editing enhances muscle function with minimal off-target effects and without elevation of systemic inflammatory cytokines. a, CRISPR–Gold improves strength and agility in *mdx* mice without CTX. A four-limb hanging test was conducted in *mdx* mice treated with CRISPR–Gold two weeks after the initial CRISPR–Gold injection. CRISPR–Gold significantly enhanced muscle strength compared with mice treated with scrambled CRISPR–Gold. Data are means ± s.e ($n = 11$ for injected *mdx* mice; $n = 6$ for control *mdx* and wild-type mice). $^{*}P < 0.05$; $^{**}P < 0.01$, compared with the scrambled CRISPR–Gold group. **b**, In vivo off-target effects were insignificant in CRISPR–Gold injected mouse muscle tissue. The major predicted and reported off-target sites for the mdx gRNA were analysed with deep sequencing. OT-01, OT-04, OT-06, OT-015, and OT-021, refer to 5 genomic DNA sequences with a high degree of complementarity to the gRNA. Control: scrambled CRISPR–Gold injection; CRISPR–Gold: CRISPR–Gold injection without CTX. Each read-out was more than 30,000 reads and all off-target mutations were within the range of deep sequencing error. **c**–**f**, CRISPR–Gold does not elevate plasma cytokine levels compared with PBS injections. Data are means ± s.e ($n = 3$). **c**,**d**, Plasma cytokine levels after a single injection of CRISPR–Gold. **e**,**f**, Plasma cytokine levels after two injections of CRISPR–Gold. **c**,**e**, High plasma level cytokines. **d**,**f**, Low plasma level cytokines. G-CSF, granulocyte-colony stimulating factor; GM-CSF, granulocyte-macrophage colony-stimulating factor; IFN, interferon; IL, interleukin; MCP, monocyte chemoattractant protein; MIP, macrophage inflammatory protein; TNF, tumour necrosis factor; KC, keratinocyte-derived chemokine.

In addition, we performed experiments in which CRISPR–Gold was injected into mice twice, three days apart. The mice were analysed for plasma cytokines and weight loss to determine whether CRISPR–Gold could be administered multiple times without toxicity. Figure 7e,f and Supplementary Fig. 25 show that CRISPR–Gold did not cause an up-regulation of inflammatory cytokines in the plasma or weight loss after multiple injections, suggesting that CRISPR–Gold can be used multiple times safely and that it has a high therapeutic window for gene editing in muscle tissue.

Outlook. We have shown that CRISPR–Gold can deliver Cas9 protein, gRNA and donor DNA—both in vitro and in vivo—and edit genes via HDR. CRISPR–Gold offers a new therapeutic strategy for treating DMD caused by point mutations and small deletions. For this class of patients, CRISPR–Gold has the potential to correct their mutation back to the wild-type sequence and regenerate fully functional wild-type dystrophin without the use of viruses. More broadly, our results demonstrate that non-viral delivery vehicles can generate HDR in vivo and have great potential for treating genetic diseases.

Methods

Please see Supplementary Tables 1–6 for a list of the DNA sequences used in this manuscript.

Materials. Oligonucleotides were purchased from Integrated DNA Technologies. GNPs (15 nm) were purchased from BBI Solutions. Sodium citrate and 4-(2-hydroxyethyl) piperazine-1-ethanesulfonate (HEPES) were purchased from Mandel Scientific. Sodium silicate and CTX (C9759) were purchased from Sigma–Aldrich. Phusion High-Fidelity DNA Polymerase was purchased from NEB. A MEGAscript T7 kit, a MEGAclear kit, PageBlue solution, propidium iodide and a PureLink Genomic DNA kit were purchased from Thermo Fisher Scientific. Mini-PROTEAN TGX Gels (4–20%) were purchased from Bio-Rad. MTeSR-1 media gentle cell dissociation reagent was purchased from STEMCELL Technologies. Matrigel was purchased from BD Biosciences. Dulbecco's Modified Eagle's medium (DMEM) media, non-essential amino acids, penicillin-streptomycin, Dulbecco's phosphate-buffered saline and 0.05% trypsin were purchased from Life Technologies. EMD Millipore Amicon Ultra-4 100 kDa was purchased from Millipore.

Expression and purification of Cas9. The full-length catalytically active *Streptococcus pyogenes* Cas9 was expressed from an expression vector previously published in a manuscript by Jinek et al.[1,2]. It was composed of a custom pET-based expression vector encoding an N-terminal 6×His-tag followed by the maltose-binding protein and a tobacco etch virus protease cleavage site, as well as two SV40 nuclear localization signal peptides at its C-terminus. Recombinant Cas9 protein was expressed in the *Escherichia coli* strain BL21 (DE3) (Novagen) and further purified to homogeneity as previously described[1,2]. Purified Cas9 protein was stored in 50 mM HEPES at pH 7.5 with 300 mM NaCl, 10% glycerol and 100 µM tris(2-carboxyethyl)phosphine at −80 °C. *S. pyogenes* Cas9 D10A nickase was expressed and purified following the same procedure[3]. The Cas9 protein concentration was determined using a NanoDrop 2000 (Thermo Fisher Scientific) from the absorbance at 280 nm.

In vitro T7 transcription of single-guide RNA (sgRNA). Oligonucleotide primers for sgRNA synthesis were purchased from IDT, with the forward primer containing a T7 promoter sequence. The DNA template for in vitro sgRNA transcription was prepared using overlapping PCR[4]. Briefly, the T7 forward template (20 nM), T7RevLong template (20 nM), T7 forward primer (1 µM) and T7 reverse primer (1 µM) were mixed with Phusion High-Fidelity DNA Polymerase (NEB) and PCR amplification was performed according to the manufacturer's protocol. RNA in vitro transcription was performed using the MEGAscript T7 kit (Thermo Fisher Scientific) and purification of the resulting RNA was conducted using the MEGAclear kit, following the manufacturer's protocol. The transcribed sgRNA was eluted into 50 mM HEPES at pH 7.5 with 300 mM NaCl, 10% (vol/vol) glycerol and 100 µM tris(2-carboxyethyl) phosphine. The concentration of sgRNA was determined using a Nanodrop 2000 Spectrophotometer (Thermo Fisher Scientific) and the final sgRNA products were stored at −80 °C for the subsequent experiments.

Synthesis of PAsp(DET). PAsp(DET) was synthesized as previously reported[5,6]. Briefly, poly(β-benzyl L-aspartate) was synthesized by the ring-opening polymerization of the β–benzyl-L-aspartate *N*-carboxy-anhydride with initiation by *n*-butylamine. The polymerization proceeded for 48 h at 37 °C under an argon atmosphere. The degree of polymerization of the benzyl-L-aspartate unit was calculated to be 55 from the ^{1}H nuclear magnetic resonance spectrum (dimethyl sulfoxide-d_6; 80 °C). The resulting poly(β-benzyl L-aspartate) was reacted with diethylenetriamine to obtain PAsp(DET). After one hour of reaction, the reaction mixture was added dropwise into cold HCl. The polymer product was purified by dialysis against 0.01 M HCl and then against deionized water overnight at 4 °C. The dialyzed solution was lyophilized to obtain the final product.

Synthesis of CRISPR–Gold. A representative synthesis of CRISPR–Gold is described in this section. GNPs (15 nm in diameter; 450 nM) were reacted with a 5′ thiol modified single-stranded oligonucleotide (DNA-SH) of 25 bases in length (200 µM), which had a region complementary to the donor DNA sequence. The reaction was performed in an Eppendorf tube in 20 mM HEPES buffer in a 100 µl volume. The NaCl concentration of the reaction was increased by 100 mM h^{-1} up to 400 mM (final volume 150 µl) by adding 1 M NaCl solution and the reaction was allowed to proceed overnight. Unconjugated DNA-SH was removed by centrifugation at 17,000 *g* for 15 min and washed two times with 20 mM HEPES buffer. The resulting GNP–DNA conjugate was hybridized with the donor oligonucleotide, generating GNP–Donor. The donor DNA (100 µM concentration; 10 µl) was added to the GNP–DNA solution in 20 mM HEPES with 50 mM NaCl (100 µl) and incubated at 65 °C for 10 minutes, then gradually brought to room temperature (−2 °C min^{-1}). The GNP–Donor solution was stored at 4 °C until further use. CRISPR–Gold was synthesized using a layer-by-layer method. Cas9 (8 µg in 10 µl) and gRNA (2 µg in 10 µl) were mixed in 80 µl of Cas9 buffer (50 mM HEPES (pH 7.5), 300 mM NaCl and 10% (vol/vol) glycerol) for 5 min at room temperature. This solution was then added to the GNP–Donor solution (0.45 pmol of GNP), generating GNP–Donor–Cas9 RNP. Freshly diluted sodium silicate (6 mM; 2 µl) was added to the GNP–Donor–Cas9 RNP solution and incubated for 5 min at room temperature. The mixture was centrifuged using an EMD Millipore Amicon Ultra-4 100 kDa at 3,000 rpm for 5 min to remove the unbound Cas9 RNP. The recovered GNP–Donor–Cas9 RNP–silicate was resuspended in 20 mM HEPES buffer (100 µl), and PAsp(DET) was added to generate a final concentration of 100 µg ml^{-1} and incubated for up to 15 min at room temperature to form the last layer of CRISPR–Gold.

Absorbance spectra, particle size (DLS and TEM) and zeta potential analysis. The synthetic intermediates in the synthesis of CRISPR–Gold, GNPs, GNP–DNA, GNP–DNA–donor DNA, GNP–Cas9 RNP and GNP–Cas9 RNP–silicate were synthesized following the protocols described in the Methods section titled "Synthesis of CRISPR-Gold" and characterized by ultraviolet-visible spectroscopy. The absorbance spectra of each sample were measured using an ultraviolet-visible spectrophotometer (NanoDrop 2000, Thermo Fisher Scientific). DLS and zeta potential measurements were also made on each intermediate at 25 °C. Zeta potential measurements were made with a Zetasizer Nano ZS instrument (Malvern Instruments), and electrophoretic mobility was measured in a folded capillary cell (DTS 1060; Malvern Instruments). The zeta potential was calculated using the Smoluchowski equation. The size of the particles measured with DLS is reported in a number-based measurement mode. Each sample was prepared and incubated for a few minutes to form particles, then transferred to the capillary cell. An equilibration time ranging from two to five minutes was needed to optimize the DLS measurements and collect accurate DLS data. TEM was conducted using a FEI Tecnai 12 microscope in the electron microscope laboratory at the University of California, Berkeley. The samples were prepared on copper TEM grids (3.05 mm; 400 mesh).

Gel electrophoresis analysis of CRISPR–Gold to determine Cas9 protein content. The ability of CRISPR–Gold to complex Cas9 was determined via gel electrophoresis following separation of the unbound Cas9 RNP from CRISPR–Gold with a spin-filter (300 K MWCO). GNP–DNA (0.45 pmol) was incubated with Cas9 (8 µg) and gRNA (2 µg) for 5 min at room temperature in 100 µl of phosphate-buffered saline (PBS). A 300 kDa concentrator (Vivaspin 500; 300 K MWCO) was used to remove the unbound components of CRISPR–Gold, and, in particular, the Cas9 and gRNA. We performed preliminary experiments and determined that both components—the Cas9 and the gRNA—flowed through the 300 kDa molecular cut-off membrane after spinning at 2,000 *g* for 3 min, and could be separated from CRISPR–Gold. After concentrating the GNP–Cas9 RNP through a 300 kDa molecular cut-off membrane, the flow through (filtrate) was collected for analysis. A similar analysis was performed on CRISPR–Gold. CRISPR–Gold without purification (the control), the flow through solution from the wash step and CRISPR–Gold after purification were analysed via gel electrophoresis. Gel electrophoresis was performed using a 4–20% Mini-PROTEAN TGX Gel (Bio-Rad) in Tris/sodium dodecyl sulfate buffer. Heparin (100 µg) was added to the CRISPR–Gold sample to dissociate the PAsp(DET) polymer from the particle to facilitate gel electrophoresis. Nucleic acid staining was conducted with SYBR Safe and then the gel was imaged with ChemiDoc MP using ImageLab software, v6.0 (http://www.bio-rad.com/en-cn/product/image-lab-software; Bio-Rad); subsequently, PageBlue solution (Thermo Fisher Scientific) staining was conducted and the gel was imaged again with the same software. The protein content in the particles was quantified via densitometry analysis on the respective gel bands. The percent binding of CRISPR–Gold was determined by comparing the amount of Cas9 present in CRISPR–Gold after purification (retentate) with the amount of Cas9 present in the unpurified CRISPR–Gold sample. Experiments were also performed to determine if GNPs by themselves (without DNA modification) bound Cas9 RNP, following the procedure described above. The percent of Cas9 RNP bound to the GNPs was determined by comparing the recovered Cas9 RNP with the amount of Cas9 RNP added to the GNPs before washing. All the Cas9 RNP binding experiments were performed in triplicate.

Enzymatic activity of Cas9 released from CRISPR–Gold. Purified samples of GNP–Cas9 RNP and CRISPR–Gold were prepared according to the procedures described in the Methods section titled "Gel electrophoresis analysis of CRISPR–Gold to determine Cas9 protein content" and incubated in 40 µl PBS containing 5 mM beta-mercaptoethanol at 37 °C for 1 h to release Cas9 from the GNPs. The particles were centrifuged at 17,000 *g* for 10 min, then 10 ul of the supernatants were collected and incubated with a PCR amplicon (200 ng) that contained a Cas9 cleavage site. After incubation at 37 °C for 2 h, the samples were analysed by gel electrophoresis using a 4–20% Mini-PROTEAN TGX Gel (Bio-Rad), stained with SYBR Safe (Thermo Fisher Scientific) and imaged with a ChemiDoc MP using ImageLab software (Bio-Rad).

BFP-expressing HEK cell culture. BFP-HEK cells were generated by infection of HEK293T cells with a BFP-containing lentivirus, followed by fluorescence-activated cell sorting (FACS)-based enrichment using the protocol published by Richardson et al.[7]. The lenti-virus was generated by transfection of HEK293FT cells with a custom lentiviral vector containing a BFP gene driven by the pEF1

promoter, cloned into a Lenti×1 DEST Blast backbone by Gateway Cloning (Life Technologies). Reporter cell lines were generated by infection of HEK293T cells with lentivirus at low multiplicity of infection (as estimated by FACS three days post-infection). BFP-positive cells were enriched by FACS, grown out and sorted into clones by FACS. A clone with high constitutive BFP fluorescence (>99% BFP positive) after expansion was selected as a reporter for BFP-GFP conversion by CRISPR–Gold-mediated HDR. To edit BFP-HEK to GFP, cells were plated at a density of 5×10^4 cells per well in a 24 well plate one day before the CRISPR–Gold experiments and cultured in DMEM with 10% fetal bovine serum, 1×MEM non-essential amino acids and 100 μg ml^{-1} penicillin-streptomycin.

Stem cell culture. Human H9 embryonic stem cells and human induced pluripotent stem cells were cultured according to the procedure described by Downing et al.[8]. Cell culture plates were coated with Matrigel diluted to 12.5 μl ml^{-1} in DMEM and incubated for one hour at 37 °C (ref. [1]). MTeSR-1 medium (STEMCELL Technologies) was added to the cells every day and the cells were passaged into 24 well plates at a density of 2×10^4 cells per well three days before Cas9 transfection. Gentle Cell Dissociation Reagent (STEMCELL Technologies) was used for cell detachment according to the manufacturer's protocol.

Mouse primary bone-marrow-derived dendritic cell culture. Bone marrow cells were obtained from the tibias and femurs of mice following the procedure of Matheu et al.[9]. Bone marrow cells were plated in complete medium containing granulocyte-macrophage colony-stimulating factor (10 ng ml^{-1}; Peprotech) for six days to allow for differentiation into dendritic cells. Cas9 transfection was conducted on day 6.

Isolation and culture of primary myoblasts from mdx mice. Primary myoblasts were obtained from C57BL/10ScSn-*Dmdmdx*/J (mdx) mice following the previously reported protocol of Conboy et al. and Rando et al.[10,11]. Briefly, the gastrocnemius and tibialis anterior muscles were harvested and incubated in collagenase for tissue dissociation. Isolated myoblasts were maintained on Matrigel-coated culture plates for a few weeks with fresh medium replacement every 24 h. The primary myoblasts were differentiated to myotubes after the CRISPR–Gold treatment. After overnight incubation with CRISPR–Gold, the medium was switched to a differentiation medium (DMEM, 2% bovine growth serum and penicillin-streptomycin) and cultured for an additional five days to allow for dystrophin expression. The myotubes were then lysed and protein was collected for western blotting.

Cell transfection. For all of the in vitro cell experiments, 10^5 cells were seeded in a 24 well plate one day before the transfection. Unless otherwise indicated, the cells in a 1 ml volume were treated with 0.45 pmol GNP–Donor (determined by absorbance), Cas9 (8 μg), gRNA (2 μg), 2 μl sodium silicate (6 mM) and 10 μg PAsp(DET). Cas9 and gRNA solution were mixed in Cas9 buffer (50 mM HEPES (pH 7.5), 300 mM NaCl and 10% (vol/vol) glycerol) for 5 min at room temperature and added to the GNP–Donor solution. Freshly diluted sodium silicate (6 mM; 2 μl) was added to the GNP solution and incubated for 5 min at room temperature. The reaction mixture was centrifuged using an EMD Millipore Amicon Ultra-4 100 kDa centrifugal filter at 3,000 rpm for 5 min to remove unbound sodium silicate. The recovered GNPs were resuspended in 20 mM HEPES buffer (100 μl), and PAsp(DET) polymer was added to produce a final concentration of 100 μg ml^{-1}, which was incubated up to 15 min at room temperature to form the last layer of CRISPR–Gold. For experiments in which less or more than 8 μg ml^{-1} of Cas9 was used, the other components of CRISPR–Gold were changed accordingly following the same ratios as described above. The CRISPR–Gold solution was added to cells to generate a final Cas9 concentration of 8 μg ml^{-1} of Cas9 protein. The cells were incubated with CRISPR–Gold in serum-free Opti-MEM for 4 h, then the medium was changed to fresh culture media (DMEM).

Nucleofection. Cells were detached by 0.05% trypsin or a gentle dissociation reagent and spun down at 600 *g* for 3 min, then washed with PBS. Nucleofection was then conducted using an Amaxa 96-well Shuttle system following the manufacturer's protocol. The nucleofection was performed in a 10 μl volume using a 100 pmol of Cas9 protein (1.6 mg/mL), 120 pmol of gRNA, and a 100 pmol of DNA-donor. The Cas9 protein was subsequently diluted to 16 μg/ ml in cell culture. The nucleofection programme was chosen to match the cell type used for the experiment. After the nucleofection, 500 μl of growth media was added and the cells were incubated at 37 °C in tissue culture plates. The cell culture media was changed 16 h after the nucleofection and the cells were incubated for a total of three days before genomic DNA extraction and analysis was conducted.

Lipofection. Lipofectamine transfection with Cas9 was performed following the protocol described by Zuris et al.[35] using 4.4 μg of Cas9, 1.2 μg of gRNA and 1.2 μl of Lipofectamine 2000 in a total volume of 100 μl (ref. [12]). Additionally, donor DNA (250 ng) was mixed with lipofectamine (500 nl) and added to the transfection media, which contained the Cas9 RNP lipofectamine solution. The lipofection was conducted in Opti-MEM media without serum and an equal volume of 2x growth media was added to the cells after 1 h of lipofection to minimize cytotoxicity. The medium was changed 16 h after the lipofection and the cells were incubated for a total of three days before genomic DNA extraction and analysis.

Flow cytometry analysis and fluorescence microscopy. Flow cytometry was used to quantify the expression levels of BFP and GFP in the BFP-HEK cells treated with CRISPR–Gold. The BFP-HEK cells were analysed seven days after Cas9 treatment. The cells were washed with PBS and detached by 0.05% trypsin. BFP and GFP expression was quantified using BD LSRFortessa X-20 and Guava easyCyte.

Sanger sequencing of the BFP/GFP gene. The GFP$^+$ population was sorted from the BFP-HEK cells that had been treated with CRISPR–Gold (seven days after treatment). Cells were detached by 0.05% trypsin treatment and the GFP$^+$-edited cells were sorted using a BD Influx cell sorter (BD Biosciences) at the Berkeley flow cytometry facility. Genomic DNA was extracted from the GFP+-sorted cells and PCR amplification of the BFP/GFP gene was conducted following the procedure described in the Methods section titled "PCR amplification of genomic DNA from transfected cells". Sanger sequencing was conducted by Quintara and the sequence was analysed using ApE software, v.2.0.51 (http://biologylabs.utah.edu/jorgensen/wayned/ape/).

PCR amplification of genomic DNA from transfected cells. Genomic DNA of 2×10^4 to 2×10^5 cells was extracted after transfection using the PureLink Genomic DNA kit (Thermo Fisher Scientific). The concentration of genomic DNA was measured using a Nanodrop 2000 (Thermo Fisher Scientific). The target genomic DNA sequences (BFP, CXCR4 and dystrophin) were amplified using primer sets and Phusion High-Fidelity DNA Polymerase or GC Buffer according to the manufacturer's protocol. All primer sets were designed to anneal outside of the homology arms of the donor DNA to avoid amplifying the donor DNA. The PCR products were analysed on a 1.5% (wt/vol) agarose gel cast with SYBR Safe (Thermo Fisher Scientific).

Analysis of genome editing efficiency with restriction enzyme digestion and Surveyor assay. HDR was determined by the restriction enzyme digestion method and indel mutations were determined by the Surveyor assay. The HDR efficiency in cells was determined with restriction enzyme digestion of PCR amplified target genes. Donor DNAs were designed to insert restriction enzyme sites, cleavable by either HindIII or DraI, into the target gene locus. The PCR amplicons of the CXCR4 and DMD loci were incubated with 10 units of HindIII and DraI, respectively. After 2–16 h of incubation at 37 °C, the products were analysed by gel electrophoresis using a 4–20% Mini-PROTEAN TGX Gel (Bio-Rad) and stained with SYBR Green (Thermo Fisher Scientific). The individual band intensity was quantified using ImageJ and the HDR efficiency was calculated using the following equation: $(b+c)/(a+b+c)\times100$, where a is the uncleaved PCR amplicon and b and c are the cleavage products. The Surveyor assay was conducted to estimate the total DNA editing (non-homologous end joining + HDR) by cutting mismatched heteroduplex DNA from mutant or HDR-modified DNA. Hybridization and Surveyor incubation were performed as described by Schumann et al.[13].

Cell viability assays. The relative cell viability of cells transfected with CRISPR–Gold, nucleofection and lipofection was determined with a Cell Counting Kit (Dojindo) using regular culture media supplemented with 10% (v/v) CCK solution. Cells were plated in a 24 well plate at a seeding density of 105 cells well–1 and the cells were treated with CRISPR–Gold as described in the Methods section titled "Cell transfection". The CCK assay was conducted two days after the transfection. Relative cell viability was defined as the percent viability compared with untreated controls.

Sanger sequencing of human embryonic stem cells edited with CRISPR–Gold. The CXCR4 PCR amplicons of CRISPR–Gold-treated human embryonic stem cells were cloned into plasmids using a Zero Blunt TOPO PCR cloning kit (Life Technologies) following the manufacturer's instruction. Briefly, TOP10 *E. coli* were transformed with plasmids containing the PCR amplicons and cultured on LB plates containing kanamycin. Sanger sequencing of the *CXCR4* gene cloned into the *E. coli* colonies was conducted by Quintara Biosciences.

Inhibitor studies with CRISPR–Gold. Cell culture experiments with various cellular uptake inhibitors and under conditions of low temperature were performed to investigate the mechanism of CRISPR–Gold uptake. L2 sgRNA was labelled with Alexa 647-NHS-ester following the method described by Lee et al.[4]. Briefly, 5′ amine modified L2 sgRNA was incubated with Alexa 647-NHS-ester (100-fold molar excess) in pH9 sodium bicarbonate buffer overnight at room temperature and purified with desalting column. CRISPR–Gold was formulated with 647-L2 sgRNA as described in the Methods section titled "Cell transfection". Wortmannin (150 ng ml^{-1}), chlorpromazine (1.5 μg ml^{-1}), genistein (5 μg ml^{-1}) and methyl-β-cyclodextrin (7.5 mg ml^{-1}) were added to HEK-293 cells for 1 h under regular culture conditions (serum). The cells were washed with PBS twice and then treated with CRISPR–Gold at a concentration of 8 μg ml^{-1} Cas9 protein. All samples were incubated at 37 °C except for the 4 °C sample, which was incubated at 4 °C for

1 h without any inhibitors. The cells were analysed 16 h after the CRISPR–Gold treatment to quantify the Alexa 647$^+$ cell population using flow cytometry.

In a separate set of experiments, BFP-HEK cells were treated with CRISPR–Gold designed to convert the BFP gene into the GFP gene via HDR. CRISPR–Gold was formulated with L2 sgRNA as described in the Methods section titled "Cell transfection". Wortmannin (150 ng ml^{-1}), chlorpromazine (1.5 μg ml^{-1}), genistein (5 μg ml^{-1}) and methyl-β-cyclodextrin (7.5 mg ml^{-1}) were added to BFP-HEK-293 cells for 1 h under regular culture conditions (serum). The cells were washed with PBS twice and then treated with CRISPR–Gold at a concentration of 8 μg ml^{-1} Cas9 protein. All samples were incubated at 37 °C. HDR efficiency was analysed three days after the treatment following the procedures described in Methods sections titled "Cell transfection" and "Flow cytometry analysis and fluorescence microscopy".

Western blot analysis for dystrophin protein production. Myoblasts were treated with CRISPR–Gold following the procedure described in the Methods section titled "Cell transfection". After differentiation, cells were harvested and protein extracts for western blot analysis were made following the procedure of Lu et al.[14]. Briefly, cells were lysed in radioimmunoprecipitation assay buffer (50 mM Tris–HCl, pH 7.4, 150 mM NaCl, 0.5% deoxycholate and 1% Nonidet P-40) containing proteinase inhibitor, and the total protein concentration was determined using a BCA Protein Assay kit (Thermo Fisher Scientific). Then, 150 μg of protein per sample was loaded onto a 4–20% gradient polyacrylamide gel (Bio-Rad, CA, Cat # 4561094) and run for 6 h at 35 volts before the protein content of the gel was transferred onto nitrocellulose membranes. The membranes were blocked with 5% milk in Tris-buffered saline plus 0.1% Tween20 followed by overnight incubation with dystrophin antibody (dilution 1 : 200, Abcam) in Tris-buffered saline plus 0.1% Tween20 to detect dystrophin. Glyceraldehyde 3-phosphate dehydrogenase (dilution 1 : 2000; Thermo Fisher Scientific) was used as a sample loading control. Blots were washed with 0.2% Tween20 in Tris-buffered saline three times and then incubated with a horseradish peroxidase-coupled secondary antibody (Azure Biosystems). Antibody binding was detected using an enhanced chemiluminescent detection system (Amersham).

In vivo delivery of CRISPR–Gold in Ai9 mice. Ai9 (Jackson Laboratory #007909) mice were purchased from Jackson Laboratory. All animal studies were performed following authorized protocols and animals were treated in accordance with the policies of the Animal Care and Use Committee of the University of California, Berkeley. Three groups of Ai9 mice were used for this experiment. The experimental groups were: control (no injection, $n=3$), CRISPR–Gold (mice injected with CRISPR–Gold, $n=3$) and positive control (Cre plasmid and lipofectamine injection, $n=1$). Each group of mice was selected randomly. Four-week-old Ai9 mice were injected in the tibialis anterior (10 μl per muscle) and gastrocnemius muscles (10 μl per muscle) using a Hamilton syringe. Two weeks after the injection, the muscles were harvested and analysed. CRISPR–Gold particles were formed as described in the Methods section titled "Synthesis of CRISPR-Gold". For all of the in vivo experiments in Ai9 mice, 6.75 pmol GNP–DNA, 120 μg Cas9 (6 mg kg^{-1} dose), 30 μg sgRNAs (15 μg of Ai9-F and 15 μg of Ai9-R), 30 μl sodium silicate (6 mM) and 150 μg PAsp(DET) were mixed and incubated for 5 min to formulate CRISPR–Gold, which was then injected into the mice. For the positive control, Cre plasmid (20 μg) and Lipofectamine 2000 (40 μl) were mixed and incubated for 10 min before the injection.

High-throughput automated imaging of a whole-muscle section. Glass slides with whole-muscle sections were imaged using a Molecular Devices ImageXpress Micro device. On average, 288 images were taken per slide with a 10x objective lens. The images were analysed using MetaXpress software, which merged the images and created a montage of the whole-muscle section.

In vivo delivery of CRISPR–Gold in mdx mice treated with CTX. Male C57BL/10ScSn (wild-type) mice and C57BL/10ScSn-*Dmdmdx*/J (mdx) mice, which contained a nonsense mutation in exon 23 of the dystrophin gene were purchased from the Jackson Laboratory. All animal studies were performed following authorized protocols and animals were treated in accordance with the policies of the Animal Care and Use Committee of the University of California, Berkeley. Three groups of mdx mice were used for this experiment. The experimental groups were: (1) control 1 (no GNP), consisting of mice injected with Cas9 RNP and donor DNA without GNPs ($n=3$), (2) control 2 (no gRNA), consisting of mice injected with CRISPR–Gold without gRNA ($n=1$) and (3) CRISPR–Gold, consisting of mice injected with CRISPR–Gold containing RNP and donor DNA ($n=3$).

Each group of mice was selected randomly. The investigators were not blinded to the group allocation during the experiment. CRISPR–Gold treatments were administered to two-month-old mdx mice via the tibialis anterior (10 μl per muscle) and gastrocnemius muscles (10 μl per muscle) using a Hamilton syringe. CRISPR–Gold particles were formed as described in the Methods section titled "Synthesis of CRISPR-Gold". For all the mdx in vivo experiments, 6.75 pmol GNP, 120 μg Cas9 (6 mg kg^{-1} dose), 30 μg gRNA, 30 μl sodium silicate (6 mM) and 150 μg PAsp(DET) were mixed and incubated for 5 min to formulate CRISPR–Gold, which was then injected into the mice. The injection mix contained CTX (0.1 mg ml^{-1}) mixed with lidocaine hydrochloride. For the no GNP control, 120 μg Cas9 (6 mg kg^{-1} dose) + 30 μg gRNA was formulated in a 10 μl volume containing CTX (0.1 mg ml^{-1}) mixed with lidocaine hydrochloride, and injected into mdx mice. The experiments were conducted in a non-blinded and non-randomized way. For the experiments with a Cas9 dose of 3 mg kg^{-1}, all of the other CRISPR–Gold reagents were scaled back accordingly. Two weeks after the injection, the mice were sacrificed and the muscles were analysed by deep sequencing and histology for dystrophin expression and fibrosis.

In vivo delivery of CRISPR–Gold in mdx mice without CTX treatment. Male C57BL/10ScSn (wild-type) mice and C57BL/10ScSn-*Dmdmdx*/J (mdx) mice, which contained a nonsense mutation in exon 23 of the dystrophin gene were purchased from the Jackson Laboratory. All animal studies were performed following authorized protocols, and animals were treated in accordance with the policies of the Animal Care and Use Committee of the University of California, Berkeley. Four groups of mice were used for this experiment. The experimental groups were: (1) negative control, consisting of mdx mice without injection ($n=6$), (2) control (scrambled CRISPR–Gold), consisting of mice injected with CRISPR–Gold containing scrambled gRNA ($n=11$), (3) CRISPR–Gold, consisting of mice injected with CRISPR–Gold containing RNP and donor DNA ($n=11$) and (4) wild-type C57BL/10ScSn mice ($n=6$).

Four-week-old mdx mice received injections in the tibialis anterior (10 μl per muscle), gastrocnemius (10 μl per muscle) and forelimb muscles (10 μl per muscle) via a Hamilton syringe. Two weeks after the injections, the mice received a second round of injections of exactly the same composition. Two weeks after the second injection, the mice were sacrificed and the muscles were analysed by deep sequencing and for dystrophin expression. A four-limb hanging test was conducted on the CRISPR–Gold-treated mdx mice at the age of six weeks, which was two weeks after the initial injection. Mice were placed on a handmade square apparatus with a grid structure. The apparatus was inverted and positioned 25 cm above the cage to discourage intentional dropping. Soft bedding was prepared to prevent the mice from harming themselves if they fell. The maximum hanging time out of three trials was recorded for a duration of 600 s. The chosen fixed hanging time limit was determined following the procedure of Aartsma-Rus et al.[15]. The wild-type mice were also tested at the age of six weeks. An unpaired Student's *t*-test was conducted using Prism 7 software v.7. The experiments were conducted in a blinded manner.

Deep sequencing analysis of CRISPR–Gold treated muscle tissue. The genomic region of the Cas9 target sequence was amplified by PCR using Phusion High-Fidelity DNA Polymerase according to the manufacturer's protocol. Target genes were amplified first with primer sets used for HDR detection and then again with deep sequencing primers to eliminate the potential for donor sequence amplification. The amplicons were purified using the ChargeSwitch PCR Clean-Up Kit (Thermo Fisher Scientific). A NEXTflex Rapid Illumina DNA-Seq Library Prep Kit was used to attach illumina adapters and PCR amplify the product for five cycles. PCR clean-up was performed one additional time. The Berkeley DNA Sequencing Facility performed DNA quantification using a Qubit 2.0 Fluorometer (Life Technologies). A Bioanalyzer was then used for size analysis and quantitative PCR. The library was sequenced with the Illumina HiSeq 2500 at the Vincent Coates Genomic Sequencing Laboratory at the University of California, Berkeley. The analysis was conducted using the CRISPR Genome Analyzer[16].

Immunofluorescence of dystrophin, CD45 and CD11b. Gastrocnemius and tibialis anterior muscles were frozen, sectioned to 10 μm and fixed with 70% ethanol at 4 °C overnight. After blocking for 1 h with 0.1% Triton X-100, slides were incubated with a primary antibody against dystrophin (Santa Cruz Biotechnology-47760 or 358922) or alternatively with anti-CD11b or anti-CD45 antibody (F10-89-4; EMD Millipore 05-1410) in PBS with 1% fetal bovine serum overnight. After three five minute washes with PBS with 1% fetal bovine serum, the slides were incubated with the respective secondary antibodies (sc-362282 from Santa Cruz Biotechnology, A11010 and A21206 from Life Technologies) for two hours at room temperature in PBS with 1% fetal bovine serum, which also contained Hoechst nuclear dye. Slides were imaged with a Zeiss Axioscope fluorescence microscope. All images were taken at 40x magnification.

C57BL/6 mice were treated with CTX and then stained for CD45 and CD11b. The procedure for treating the C57BL/6 mice with CTX is described below. Mice were anaesthetized with isoflurane and the hind leg muscles (tibialis anterior and/or gastrocnemius) were injured percutaneously with 5–10 μl CTX-1 (1 mg ml^{-1}; Sigma–Aldrich). Typically, such small focal injuries completely heal in five days. The animals were monitored for general signs of health (for example, activity and inquisitiveness) and the regeneration site (for example, the leg) was examined for signs of tissue damage or necrosis (which did not occur).

Trichrome staining. Muscle sections were stained using a Gomori Trichrome Stain Kit (Polysciences #24205-1) according to the manufacturer's instructions. Briefly, ethanol-fixed sections were fixed again overnight at room temperature in Bouin's fixative, then stained with Weigert's iron haematoxylin, then with

Gomori trichrome stain and finally with 1% acetic acid. Clearing and mounting steps were then performed with dehydration.

PCR amplification of genomic DNA from CRISPR–Gold-edited muscle tissue. Muscle genomic DNA from either control mice (Cas9 RNP + donor DNA without GNP) or CRISPR–Gold-treated mice was amplified with primers designed to only amplify the HDR-edited sequence. PCR was conducted using the forward primer (AAAGGAGCAGCAGAATGGCT), reverse primer (CCACCAACTGGGAGGAAAG) and Phusion High-Fidelity PCR Master Mix with GC Buffer according to the manufacturer's protocol. The PCR products were analysed on a 1.5% (wt/vol) agarose gel casted with SYBR Safe (Thermo Fisher Scientific).

Off-target deep sequencing analysis. Deep sequencing was performed on CRISPR–Gold-treated mdx mice (without CTX) to investigate the frequency of off-target genomic damage. Potential off-target loci were determined using CRISPR off-target prediction programmes, which were identical to the off-target loci identified by Long et al.[17]. PCR was conducted using the primers listed in the Supplementary Tables 1–6. The amplicons were purified using the ChargeSwitch PCR Clean-Up kit (Thermo Fisher Scientific). The NEXTflex Rapid Illumina DNA-Seq Library Prep Kit was used to attach illumina adapters and PCR amplify the product for five cycles. PCR clean-up was then performed a second time. DNA quantification was performed at the Berkeley DNA Sequencing Facility using a Qubit 2.0 Fluorometer (Life Technologies). A Bioanalyzer was used for size analysis, followed by quantitative PCR. The library was sequenced using the Illumina HiSeq 2500 at the Vincent Coates Genomic Sequencing Laboratory at University of California, Berkeley, using the 150PE read. The analysis was conducted using the CRISPR Genome Analyzer (54.80.152.219). Figure 7b in the main manuscript presents the off-target mutation frequency of control and the CRISPR–Gold-injected mouse samples (without CTX).

Bio-Plex cytokine assay and weight loss. Systemic inflammation and toxicity induced by CRISPR–Gold was assessed by measuring the concentrations of 22 murine cytokines, as well as weight loss, in mice that had been injected with CRISPR–Gold. The plasma cytokine concentrations were measured using Bio-Plex kits (Bio-Rad; Cat# M60009RDPD). CRISPR–Gold-mediated inflammation was assayed under three different conditions. Under condition 1, mice received a single CRISPR–Gold injection and were sacrificed after 24 h. Condition 2 was the same as condition 1 only mice were sacrificed after two weeks. In condition 3, mice received two CRISPR–Gold injections three days apart and were sacrificed 24 h after the second injection. Following all conditions, plasma cytokines and weight loss were measured.

For each condition, the mice received either control PBS or CRISPR–Gold ($n = 3$ for each group). The CRISPR–Gold contained a dose of 6 mg kg^{-1} of Cas9 protein per injection. Each injection delivered a volume of 10 µl to the gastrocnemius or tibialis anterior muscle following the method described in the Methods section titled "In vivo delivery of CRISPR–Gold in mdx mice without CTX treatment". The assays were run according to manufacturer's recommended procedures. The plates were read in a Bio-Plex 200 System and the data were analysed using Bio-Plex Manager 4.1 software (http://www.bio-rad.com/en-us/product/bio-plex-manager-software-standard-edition). The assays were performed in duplicate and all data points were analysed except for one cytokine that was not detected in the assay.

Statistical analyses. Statistical analyses were conducted using Graphpad's Prism7 software. A Student's *t*-test was conducted for two-sample analyses and a one-way analysis of variance with post-hoc Tukey's honest significant difference was conducted for multiple sample analyses.

Data availability. The data that support the findings of this study are available within the paper and its Supplementary Information.

Received: 4 January 2017; Accepted: 22 August 2017;
Published online: 02 October 2017

References

1. Jinek, M. et al. A programmable dual-RNA-guided DNA endonuclease in adaptive bacterial immunity. *Science* **337**, 816–822 (2012).
2. Cong, L. et al. Multiplex genome engineering using CRISPR/Cas system. *Science* **339**, 819–823 (2013).
3. Mali, P. et al. RNA-guided human genome engineering via Cas9. *Science* **339**, 823–826 (2013).
4. Cho, S. W., Kim, S., Kim, J. M. & Kim, J.-S. Targeted genome engineering in human cells with the Cas9 RNA-guided endonuclease. *Nat. Biotechnol.* **31**, 230–232 (2013).
5. Ran, F. A. et al. *In vivo* genome editing using *Staphylococcus aureus* Cas9. *Nature* **520**, 186–190 (2015).
6. Yin, H. et al. Therapeutic genome editing by combined viral and non-viral delivery of CRISPR system components *in vivo*. *Nat. Biotechnol.* **34**, 328–333 (2016).
7. Schumann, K. et al. Generation of knock-in primary human T cells using Cas9 ribonucleoproteins. *Proc. Natl Acad. Sci. USA* **112**, 201512503 (2015).
8. Lin, S., Staahl, B., Alla, R. K. & Doudna, J. A. Enhanced homology-directed human genome engineering by controlled timing of CRISPR/Cas9 delivery. *Elife* **3**, 1–13 (2014).
9. Tabebordbar, M. et al. In vivo gene editing in dystrophic mouse muscle and muscle stem cells. *Science* **351**, 407–411 (2016).
10. Nelson, C. E. et al. In vivo genome editing improves muscle function in a mouse model of Duchenne muscular dystrophy. *Science* **351**, 403–407 (2016).
11. Long, C. et al. Postnatal genome editing partially restores dystrophin expression in a mouse model of muscular dystrophy. *Science* **351**, 400–403 (2016).
12. Dever, D. P. et al. CRISPR/Cas9 β-globin gene targeting in human haematopoietic stem cells. *Nature* **539**, 384–389 (2016).
13. Yin, H. et al. Genome editing with Cas9 in adult mice corrects a disease mutation and phenotype. *Nat. Biotechnol.* **32**, 551–553 (2014).
14. Lu, Q. L. et al. Systemic delivery of antisense oligoribonucleotide restores dystrophin expression in body-wide skeletal muscles. *Proc. Natl Acad. Sci. USA* **102**, 198–203 (2005).
15. Sun, W. et al. Self-assembled DNA nanoclews for the efficient delivery of CRISPR-Cas9 for genome editing. *Angew. Chem. Int. Ed. Engl.* **54**, 12029–12033 (2015).
16. Kim, S., Kim, D., Cho, S. W., Kim, J. & Kim, J. S. Highly efficient RNA-guided genome editing in human cells via delivery of purified Cas9 ribonucleoproteins. *Genome Res.* **24**, 1012–1019 (2014).
17. Ramakrishna, S. et al. Gene disruption by cell-penetrating peptide-mediated delivery of Cas9 protein and guide RNA. *Genome Res.* **24**, 1020–1027 (2014).
18. Yu, X. et al. Improved delivery of Cas9 protein/gRNA complexes using lipofectamine CRISPRMAX. *Biotechnol. Lett.* **38**, 919–929 (2016).
19. Miyata, K. et al. Polyplexes from poly(aspartamide) bearing 1,2-diaminoethane side chains induce pH-selective, endosomal membrane destabilization with amplified transfection and negligible cytotoxicity. *J. Am. Chem. Soc.* **130**, 16287–16294 (2008).
20. Kim, H. J. et al. Introduction of stearoyl moieties into a biocompatible cationic polyaspartamide derivative, PAsp(DET), with endosomal escaping function for enhanced siRNA-mediated gene knockdown. *J. Control. Release* **145**, 141–148 (2010).
21. Ding, Y. et al. Gold nanoparticles for nucleic acid delivery. *Mol. Ther.* **22**, 1075–1083 (2014).
22. Singh, D., Sternberg, S. H., Fei, J., Ha, T. & Doudna, J. A. Real-time observation of DNA recognition and rejection by the RNA-guided endonuclease Cas9. *Nat. Commun.* **7**, 1–8 (2016).
23. Sternberg, S. H., Redding, S., Jinek, M., Greene, E. C. & Doudna, J. A. DNA interrogation by the CRISPR RNA-guided endonuclease Cas9. *Nature* **507**, 62–67 (2014).
24. Walkey, C. D. et al. Protein corona fingerprinting predicts the cellular interaction of gold and silver nanoparticles. *ACS Nano* **8**, 2439–2455 (2014).
25. Liu, J. & Peng, Q. Protein-gold nanoparticle interactions and their possible impact on biomedical applications. *Acta Biomater.* **55**, 13–27 (2017).
26. Chithrani, B. D., Ghazani, A. A. & Chan, W. C. W. Determining the size and shape dependence of gold nanoparticle uptake into mammalian cells. *Nano Lett.* **6**, 662–668 (2006).
27. Chou, L. Y. T., Zagorovsky, K. & Chan, W. C. W. DNA assembly of nanoparticle superstructures for controlled biological delivery and elimination. *Nat. Nanotechnol.* **9**, 148–155 (2014).
28. Rouge, J. L., Hao, L., Wu, X. A., Briley, W. E. & Mirkin, C. A. Spherical nucleic acids as a divergent platform for synthesizing RNA–nanoparticle conjugates through enzymatic ligation. *ACS Nano* **8**, 8837–8843 (2014).
29. Smith, R. C., Riollano, M., Leung, A. & Hammond, P. T. Layer-by-layer platform technology for small-molecule delivery. *Angew. Chem. Int. Ed. Engl.* **48**, 8974–8977 (2009).
30. Fu, Y., Sander, J. D., Reyon, D., Cascio, V. M. & Joung, J. K. Improving CRISPR-Cas nuclease specificity using truncated guide RNAs. *Nat. Biotechnol.* **32**, 279–284 (2014).
31. Richardson, C. D., Ray, G. J., DeWitt, M. A., Curie, G. L. & Corn, J. E. Enhancing homology-directed genome editing by catalytically active and inactive CRISPR-Cas9 using asymmetric donor DNA. *Nat. Biotechnol.* **34**, 339–344 (2016).
32. Lee, K. et al. Synthetically modified guide RNA and donor DNA are a versatile platform for CRISPR-Cas9 engineering. *Elife* **6**, e25312 (2017).
33. Yang, L. et al. Optimization of scarless human stem cell genome editing. *Nucleic Acids Res.* **41**, 9049–9061 (2013).
34. Long, C. et al. Prevention of muscular dystrophy in mice by CRISPR/Cas9-mediated editing of germline DNA. *Science* **345**, 1184–1188 (2014).
35. Zuris, J. A. et al. Cationic lipid-mediated delivery of proteins enables efficient protein-based genome editing *in vitro* and *in vivo*. *Nat. Biotechnol.* **33**, 73–80 (2014).

36. Hegde, M. R. et al. Microarray-based mutation detection in the dystrophin gene. *Hum. Mutat.* **29**, 1091–1099 (2008).
37. Nakamura, A. & Takeda, S. Exon-skipping therapy for Duchenne muscular dystrophy. *Lancet* **378**, 546–547 (2011).
38. Mendell, J. R. et al. Eteplirsen for the treatment of Duchenne muscular dystrophy. *Ann. Neurol.* **74**, 637–647 (2013).
39. Kornegay, J. N. et al. Widespread muscle expression of an AAV9 human mini-dystrophin vector after intravenous injection in neonatal dystrophin-deficient dogs. *Mol. Ther.* **18**, 1501–1508 (2010).
40. Xu, L. et al. CRISPR-mediated genome editing restores dystrophin expression and function in mdx mice. *Mol. Ther.* **24**, 564–569 (2016).
41. Pavlath, G. K. & Horsley, V. Cell fusion in skeletal muscle—central role of NFATC2 in regulating muscle cell size. *Cell Cycle* **2**, 420–423 (2003).
42. Sy, J. C. et al. Sustained release of a p38 inhibitor from non-inflammatory microspheres inhibits cardiac dysfunction. *Nat. Mater.* 863–869 (2008).

Acknowledgements

This work was supported by grants from the National Institutes of Health (U01 268201000043C-0-0-1 and R56 AI107116-01 to I.C. as well as grants from Calico, Roger's and the Strategies for Engineered Negligible Senescence Research Foundation to I.C. This work was also supported by the W. M. Keck Foundation, Moore Foundation, Li Ka Shing Foundation and Center of Innovation programme of the Japan Science and Technology Agency. K.L. is a Siebel Fellow of the Siebel Scholars Foundation. F.J. is a Merck Fellow of the Damon Runyon Cancer Research Foundation (DRG-2201-14). M.A.D. is a California Institute for Regenerative Medicine (CIRM) post-doctoral fellow and is supported by CIRM training grant TG2-01164. J.A.D is a Howard Hughes Medical Institute Investigator. We thank M. West at the CIRM/QB3 Shared Stem Cell Facility and H. Nolla and T. Shovha at the Berkeley FACS facility for technical assistance, as well as D. Schaffer, L. S. Qi, B. Staahl, S. Lin and S. Yang for advice and technical support. This work used the Vincent J. Coates Genomics Sequencing Laboratory at the University of California, Berkeley, supported by National Institutes of Health S10 Instrumentation Grants S10RR029668 and S10RR027303.

Author contributions

K.L. planned and performed the experiments shown in all the figures, analysed and interpreted the data and wrote the manuscript. M.C. designed, planned and performed the in vivo studies shown in Figs. 5 and 6 and wrote the manuscript. H.M.P. and H.L. performed the in vivo experiments and analysed and interpreted the data. F.J. purified the Cas9 protein and analysed the gel data. H.J.K. and K.K. synthesized the PAsp(DET) polymer, performed the experiment shown in Supplementary Table 1 and contributed to the data interpretation. W.-c.H. and S.L. cultured the stem cells and performed the experiment shown in Supplementary Fig. 7. M.A.D. and J.E.C. generated the BFP-HEK cells and supported the deep sequencing analysis. V.A.M., K.C., H.M.P. and A.R. performed the in vitro and in vivo DNA analysis. C.S., M.M. and T.S. performed the muscle histology studies. F.L. and N.L.B. performed the deep sequencing analysis. J.E.C. and J.A.D. contributed to the design of the studies and data interpretation. I.C. and N.M. planned and integrated the work, interpreted the data and wrote the manuscript.

Competing interests

K.L., H.M.P. and N.M. are co-founders of GenEdit. J.A.D. is a co-founder of Caribou Biosciences, Editas Medicine and Intellia Therapeutics.

Additional information

Supplementary information is available for this paper at doi:10.1038/s41551-017-0137-2.

Correspondence and requests for materials should be addressed to I.C. or N.M.

nature research

Corresponding author(s): Niren Murthy

☐ Initial submission ☐ Revised version ☒ Final submission

Life Sciences Reporting Summary

Nature Research wishes to improve the reproducibility of the work that we publish. This form is intended for publication with all accepted life science papers and provides structure for consistency and transparency in reporting. Every life science submission will use this form; some list items might not apply to an individual manuscript, but all fields must be completed for clarity.

For further information on the points included in this form, see Reporting Life Sciences Research. For further information on Nature Research policies, including our data availability policy, see Authors & Referees and the Editorial Policy Checklist.

Experimental design

1. Sample size

Describe how sample size was determined.

No statistical methods were used to predetermine or justify sample sizes, but our sample sizes are similar to those generally employed in the field.

2. Data exclusions

Describe any data exclusions.

The only excluded data point is in supplementary figure 21. IL-9 was excluded because the cytokine values from both samples were lower than the detection limit of the assay.

3. Replication

Describe whether the experimental findings were reliably reproduced.

Each experiment was replicated multiple times, and the replication numbers are listed in the methods.

4. Randomization

Describe how samples/organisms/participants were allocated into experimental groups.

Control and injected mice were chosen randomly. We randomized the injection side (left or right leg) per experiment.

5. Blinding

Describe whether the investigators were blinded to group allocation during data collection and/or analysis.

The investigator was not blinded to the group allocation during the experiment and when assessing the outcome.

Note: all studies involving animals and/or human research participants must disclose whether blinding and randomization were used.

6. Statistical parameters

For all figures and tables that use statistical methods, confirm that the following items are present in relevant figure legends (or in the Methods section if additional space is needed).

n/a	Confirmed	
☐	☒	The exact sample size (*n*) for each experimental group/condition, given as a discrete number and unit of measurement (animals, litters, cultures, etc.)
☐	☒	A description of how samples were collected, noting whether measurements were taken from distinct samples or whether the same sample was measured repeatedly
☐	☒	A statement indicating how many times each experiment was replicated
☐	☒	The statistical test(s) used and whether they are one- or two-sided (note: only common tests should be described solely by name; more complex techniques should be described in the Methods section)
☐	☒	A description of any assumptions or corrections, such as an adjustment for multiple comparisons
☐	☒	The test results (e.g. *P* values) given as exact values whenever possible and with confidence intervals noted
☐	☒	A clear description of statistics including central tendency (e.g. median, mean) and variation (e.g. standard deviation, interquartile range)
☐	☒	Clearly defined error bars

See the web collection on statistics for biologists for further resources and guidance.

Software

Policy information about availability of computer code

7. Software

Describe the software used to analyze the data in this study.	Prism, Imagelab, ImageJ, and ZEN, among others. They are listed in the Methods section.

For manuscripts utilizing custom algorithms or software that are central to the paper but not yet described in the published literature, software must be made available to editors and reviewers upon request. We strongly encourage code deposition in a community repository (e.g. GitHub). *Nature Methods* guidance for providing algorithms and software for publication provides further information on this topic.

Materials and reagents

Policy information about availability of materials

8. Materials availability

Indicate whether there are restrictions on availability of unique materials or if these materials are only available for distribution by a for-profit company.	There are no restrictions on materials availability.

9. Antibodies

Describe the antibodies used and how they were validated for use in the system under study (i.e. assay and species).	Primary antibody against dystrophin (Santa Cruz Biotechnology-47760 or 358922). Secondary antibody (Santa Cruz Biotechnology-2005 or 362282). Anti-CD45 Antibody, clone F10-89-4, EMD Millipore 05-1410.

10. Eukaryotic cell lines

a. State the source of each eukaryotic cell line used.	BFP-HEK293T cells from the lab of Jacob E. Corn at UC Berkeley.
b. Describe the method of cell line authentication used.	No eucaryotic cell lines were used.
c. Report whether the cell lines were tested for mycoplasma contamination.	Mycoplasma test was conducted and the result was negative.
d. If any of the cell lines used are listed in the database of commonly misidentified cell lines maintained by ICLAC, provide a scientific rationale for their use.	No commonly misidentified cell lines were used.

Animals and human research participants

Policy information about studies involving animals; when reporting animal research, follow the ARRIVE guidelines

11. Description of research animals

Provide details on animals and/or animal-derived materials used in the study.	Male C57BL/10ScSn, Ai9(RCL-tdT), and C57BL/10ScSn-Dmdmdx/J (mdx) mice were purchased from the Jackson Laboratory. 3-8 week-old mice. All animal studies were performed following authorized protocols, and animals were treated in accordance with the policies of the animal ethics committee of the University of California at Berkeley.

Policy information about studies involving human research participants

12. Description of human research participants

Describe the covariate-relevant population characteristics of the human research participants.	The study did not involve human research participants.